Published in final edited form as:
Chem Soc Rev. 2011 December ; 40(12): 5771–5788. doi:10.1039/c1cs15014f.

Pyrene-functionalized oligonucleotides and locked nucleic acids (LNAs): Tools for fundamental research, diagnostics, and materials science†

Michael E. Østergaard and **Patrick J. Hrdlicka**

Abstract

Pyrene-functionalized oligonucleotides (PFOs) are increasingly explored as tools in fundamental research, diagnostics and materials science. Their popularity is linked to the ability of pyrenes to function as polarity-sensitive and quenchable fluorophores, excimer-generating units, aromatic stacking moieties and nucleic acid duplex intercalators. These characteristics have motivated development of PFOs for detection of complementary DNA/RNA targets, single nucleotide polymorphisms (SNPs), and generation of π-arrays on nucleic acid scaffolds. This *Review* will highlight the physical properties and applications of PFOs that are likely to provide *high degree of positional control* of the chromophore in nucleic acid complexes. Particular emphasis will be placed on *pyrene-functionalized Locked Nucleic Acids (LNAs)* since these materials display distinctive properties such as large fluorescence quantum yields, efficient discrimination of SNPs, and recognition of mixed-sequence double stranded DNA.

1. Introduction

Development of pyrene-functionalized oligonucleotides (PFOs) is a research area that enjoys considerable attention. A simple Web of Science search using the terms “oligonucleotide and pyrene”, reveals that more than 230 original research articles have appeared on this topic since 2005. The motivation for this work ranges from a desire to obtain a deeper fundamental understanding of nucleic acid structures over to the prospect of developing enabling tools for wide-ranging applications in materials science, diagnostics and therapeutics. Representative applications include a) generation of self-assembled helical chromophore arrays with distinct photochemical and `communication' properties, b) specific detection of complementary DNA/RNA and single nucleotide polymorphisms (SNPs), and c) targeting of mixed-sequence double stranded DNA.

This *Review* will highlight PFOs that are likely to offer a *high degree of positional control* of the chromophore in nucleic acid complexes as these materials display properties which are difficult to mimic with more flexible analogs. Considerable emphasis will be placed on *pyrene-functionalized LNAs (Locked Nucleic Acids)*, i.e., oligodeoxyribonucleotides (ONs) modified with monomers where pyrene moieties are attached via short linkers to LNA or analogs hereof, since higher *positional control* of the label is expected. The properties of oligonucleotides composed of non-nucleosidic pyrene-functionalized monomers are not covered herein and the reader is directed to recent reviews instead.[1–3]

†Part of a themed issue on the advances in DNA-based nanotechnology

Department of Chemistry, University of Idaho, Moscow, ID-83844, USA. Fax:+1 208 885 6173; Tel:+1 208 885 0108; hrdlicka@uidaho.edu.

The Review is structured to provide: a) a physicochemical background to assist interpretation of key experimental observations with PFOs, b) an overview of pyrene-functionalized nucleotide monomers and their hybridization properties, and c) an introduction to LNA and overview of pyrene-functionalized LNA monomers. This then sets the stage for a survey of recent PFO-based applications.

2. Characteristics of pyrene moieties in nucleic acid contexts

The surface area of the aromatic pyrene moiety (Fig. 1) is comparable to that of Watson-Crick base pairs (stacking area: pyrene ~184 $Å^2$, A:T base pair ~223 $Å^2$).[4] As a result, pyrene moieties have a tendency to π-stack with aromatic units (nucleobases and/or other pyrene moieties) and, accordingly, to intercalate into DNA homoduplexes. The latter results in local unwinding of the duplex by ~3.4 Å, bathochromic pyrene absorption shifts, increased probability of fluorescence quenching due to increased interactions with nucleobases (*vide infra*), and increased duplex thermostability (i.e., increased thermal denaturation temperature T_m).[5] Pyrene moieties exhibit a lower tendency for intercalation into *A*-type duplexes than into *B*-typew compressed and have less efficient nucleobase overlap.[6]

The absorption spectrum of pyrene exhibits maxima at 275, 320 and 337 nm in deoxygenated CH_2Cl_2. The corresponding fluorescence emission spectrum exhibits five maxima (372, 378, 383, 393 and 413 nm); however, only vibronic bands I and III are typically observed due to signal broadening.[7] The relative ratio of vibronic bands I and III is sensitive to solvent polarity, e.g., higher I_{III}/I_I-ratios are observed in apolar environments.[8] This sensitivity can indicate the position of pyrene labels in nucleic acid duplexes due to differential polarities of the minor/major groove (more polar) and duplex core (more apolar). Nearby nucleobase moieties can quench pyrene fluorescence via photoinduced electron transfer (PET). Guanine moieties are regarded the strongest quenchers (via oxidative electron transfer from guanine); cytosine, and to a lesser degree, thymine are considered moderately strong quenchers via reductive electron transfer to nucleobase, while adenine is a weak quencher.[9–11] Thus, higher fluorescence emission quantum yields Φ_F (i.e., ratio of photons emitted as fluorescence relative to absorbed photons) are expected when a pyrene moiety is located in the polar grooves, than when intercalated in a GC-rich duplex core (Fig. 1).

Pyrene chromophores may display excimer fluorescence when a pyrene in an electronically excited state forms a π-stacking dimer with a pyrene in its ground state.[12] Excimer emission is broad, featureless, and markedly red-shifted (λ_{em} ~490 nm) relative to pyrene monomer fluorescence. Formation of pyrene excimers can be exploited diagnostically and yield valuable structural information as the co-planar pyrenes must be separated by ~3.4 Å for efficient excimer formation (Fig. 1).

Development of modified pyrene fluorophores with red-shifted absorption and fluorescence emission maxima is desirable to minimize auto-fluorescence of biomolecules during in vivo applications. The photophysical properties of pyrene are easily modulated by direct electronic coupling to a nucleobase moiety or by extending π-conjugation. Electronic coupling to a nucleobase is most easily achieved by direct attachment of a pyren-1-yl moiety to the 5-position of 2'-deoxyuridine (**2**, Fig. 2). Excitation of the pyrene results in charge-transfer to the nucleobase giving a broad, red-shifted and solvent dependent emission band (λ_{em} ~495 nm).[13] While 8-(pyren-1-yl)-2'-deoxyguanosine monomer **9** also displays electronic coupling (λ_{em} ~460 nm),[14] attachment of pyren-1-yl to the C5-position of 2'-deoxycytidine[15] or of pyren-2-yl to the C5-position of 2'-deoxyuridine does not.[16] Electronic coupling to a nucleobase can also occur through unsaturated linkers; 5-(1-

ethynylpyrenyl)-2'-deoxyuridine and 8-(1-ethynylpyrenyl)-2'-deoxyadenosine monomers **3** and **11** display bathochromic shifts in UV absorption and unstructured fluorescence emission (λ_{em} ~450 nm) due to exciplex formation between the pyrene and nucleobase moieties (Fig. 2). Interestingly, 5-(1-ethynylpyrenyl)-2'-deoxycytidine or 8-(1-ethynylpyrenyl)-2'-deoxyguanosine **12** do not result in electronic coupling.[17]

Extension of π-conjugation through alkyne substitution is another approach to modulate the photophysical properties of pyrene moieties.[18–19] For example, attachment of two phenylethynyl moieties at different positions on pyrene results in marked bathochromic shifts in absorption (up to 40 nm) and fluorescence emission (up to 80 nm) relative to mono-substituted pyrene derivatives.[19]

3. Pyrene-functionalized nucleotide monomers

Pyrene moieties can be linked to nucleosides: a) by replacing the nucleobase moiety, b) through attachment to the nucleobase moiety, and c) through attachment to the sugar moiety. The attachment point and linker length influence the position and characteristics of the pyrene label within a nucleic acid duplex. An overview of major PFO classes is provided in the following subsections along with a brief discussion of their hybridization properties and likely pyrene binding modes. The Reader should note that direct comparison of relative effects on duplex thermostability upon incorporation of different pyrene-functionalized monomers is not possible due to sequence-dependent effects and the lack of a consensus set of model targets. Moreover, the discussion of binding modes predominantly relies on indirect structural data (e.g., fluorescence emission spectra and molecular modeling) as direct structural data (e.g., NMR structures) only has been reported in few cases.

3.1 Monomers with nucleobase surrogates

Substitution of the nucleobase with a pyrene, positions the aromatic moiety into the base stack of nucleic acid duplexes. DNA duplexes that are singly modified with monomer 1 are destabilized relative to unmodified duplexes due to local disruption of Watson-Crick base pairing (ΔT_m = −7 to −5 °C), and display universal base behavior, i.e., almost identical T_m-values regardless of the nucleotide opposite to the modification.[20] The latter, most likely, reflects the ability of the pyrene moiety to provide a π-stacking surface comparable to a Watson-Crick base pair and to partially flip out the opposing nucleobase from the duplex core (*vide infra*).

3.2 Nucleobase-modified monomers

Numerous building blocks have been developed where pyrene moieties are attached to the C5-position of pyrimidines or C8-position of purines (Fig. 2). The synthesis of these monomers is relatively straightforward and involves palladium-catalyzed cross couplings (i.e., Sonogashira, Heck, Suzuki-Miyaura) on C5-halogenated pyrimidines or C8-halogenated purines as the key step. Pyrene moieties can, alternatively, be introduced via Cu (I) catalyzed azide alkyne Huisgen 1,3-dipolar cycloadditions on C5-ethynyl-modified pyrimidines to give triazole-linked pyrene-functionalized nucleotides.[21] Small C5-substituents such as propyn-1-yl and 3-aminopropyn-1-yl, point toward the major groove of duplexes leading to considerable increases in thermal denaturation temperature relative to unmodified ONs (ΔT_m/modification ~4 °C).[22,23] Larger, more hydrophobic C5-substituents such as pyrene moieties that are attached via short rigid linkers as in **2–4**, **6** and **8** (Fig. 2), typically result in markedly decreased duplex thermostability.[21,24–26] Molecular modeling studies and fluorescence data (*vide infra*) suggest that the nucleobase of **4** adopts an *anti* conformation (Watson-Crick base pairing orientation) to position the pyrene in the major groove upon hybridization with complementary DNA, while adopting a *syn* conformation

upon hybridization to mismatched DNA, which putatively results in pyrene intercalation.[26] This binding mode is also likely when long flexible linkers are used as in monomers **5** and **7** (Fig. 2), which results in markedly increased duplex thermostability (ΔT_m/mod +7 to +10 °C).[24,27]

C8-pyrene-functionalized purine monomers with short linkers between the pyrene and nucleobase moieties greatly destabilize DNA duplexes presumably since *syn*-conformations are adopted (e.g., **9**, Fig. 2).[14] The use of a more flexible linker (e.g. **14**, Fig. 2) stabilizes DNA duplexes although the pyrene binding mode is not clear.[28]

C7-functionalized 7-deazapurines are well-tolerated in duplexes when carrying small substituents, leading to the hypothesis that these monomers predominantly adopt *anti*-conformations to place C7-substituents in the major groove.[29] It is therefore surprising that only few C7-pyrene-functionalized 7-deazapurines have been reported in literature (e.g. **15** and **16**, Fig. 2).[30–31] Incorporation of monomer **16** into a 13-mer DNA sequence results in increased duplex thermostability (ΔT_m/mod = +3.0 °C).[30]

3.3 Sugar-modified monomers

The furanose ring has been widely explored as an attachment site for pyrene moieties. Incorporation of C1'-pyrene-functionalized monomer **17** into ONs, obtained through post-synthetic conjugation of HBTU/HOBT-activated pyrene butyric acid with 1'-aminomethylthymidine under microwave conditions, increases DNA duplex thermostability (ΔT_m/mod up to +3.5 °C/mod). Molecular modeling studies suggest that the substituent points toward the minor groove although intercalation cannot be excluded due to the flexible linker.[32]

Monomers **27**[33] and **28**[34] are two prominent examples of C4'-pyrene-functionalized monomers, which are obtained by post-synthetic conjugation of activated pyrene-1-carboxylic acid with 4'-amino methylthymidine and 4'-piperazinomethylthymidine, respectively (Fig. 2). Incorporation of monomer **27** into ONs only has a minor effect on DNA duplex thermostability, presumably because the pyrene moiety is directed toward the minor groove. Hybridization of DNA strands with mismatched nucleotides opposite of monomer **27** only leads to moderately decreased duplex thermostability suggesting an intercalative binding mode of the pyrene moiety, which is substantiated by fluorescence experiments (*vide infra*).[33] Incorporation of the piperazino analog **28** into ONs results in markedly increased thermal affinity toward DNA (ΔT_m ~ +7 °C) and decreased thermal affinity toward RNA complements (ΔT_m ~ −8 °C).[34] The pronounced DNA-selectivity suggests an intercalative binding mode of the pyrene moiety, while the excellent mismatch discrimination and fluorescence data indicate a minor groove binding mode.

The 2'-position on the sugar ring has been a rigorously studied site for attachment of pyrene moieties. Single incorporation of 2'-*O*-(pyren-1-yl)methyluridine monomer **21** into DNA strands results in stabilization of DNA:DNA duplexes, the extent of which greatly depends on whether a pyrimidine (ΔT_m = ~2 °C) or purine (ΔT_m = 7–13 °C) is flanking the modification on the 3'-side (Fig. 2).[35] Modified DNA:RNA duplexes are strongly destabilized and display similar sequence dependence (Δ_{Tm} = −10 °C to −1 °C).[35] Incorporation of a single monomer **21** into RNA strands leads to minor stabilization of RNA:DNA duplexes (ΔT_m = 0 to +3 °C) and destabilization of RNA:RNA duplexes (ΔT_m = −3 to −4 °C).[36] NMR studies demonstrate that the pyrene moiety predominantly points into the minor groove in RNA:RNA duplexes, while it is intercalated toward the 3'-side in DNA:DNA duplexes indicating that the abovementioned sequence-dependent hybridization properties are linked to the π-stacking surface size of the 3'-flanking nucleotide.[37] These

characteristics of **21** have been used to develop hybdridization probes for detection of specific RNA targets (*vide infra*).[36]

Korshun and coworkers studied a series of pyrene-functionalized 2'-carbamate monomers, which are obtained from the free nucleoside via a robust six step reaction sequence featuring a carbonyldiimidazole-activated carbamate formation as the key step.[38–39] The effects upon incorporation of *ribo*-configured monomer **22** (Fig. 2) into DNA strands range from moderately increased to moderately decreased thermal affinity toward complementary DNA/RNA. The pyrene moiety is presumably located in the minor groove but structural evidence has not been obtained.[38–39] Incorporation of the corresponding *arabino*-configured monomers **18–20** (Fig. 2) into DNA strands leads to markedly reduced thermostability of duplexes with DNA complements (ΔT_m = −2 to −8 °C). Molecular modeling indicates that the pyrene moiety is located in the major groove.[40–41]

N2'-functionalization of 2'-amino-DNA analogs has been another popular approach toward introduction of pyrene moieties. The key synthetic step involves chemoselective *N*-alkylation or *N*-acylation of 2'-amino-DNA intermediates. Single incorporation of pyrene-functionalized monomers **23**[42], **24**[43], **25**[44] or **26**[44] into 5'-d(GTG A**B**A TGC) leads to pronounced increases in DNA:DNA duplex thermostability (vs DNA: ΔT_m = +3, +15, +3, and +6 °C, respectively). The strong DNA-selectivity of these monomers (vs RNA: ΔT_m = −6, +2, −8, and +1 °C, respectively), along with data from fluorescence spectroscopy, indicates that the pyrene binding mode is similar as for the previously discussed 2'-*O*-(pyren-1-yl)methyluridines, i.e., intercalation upon hybridization with DNA targets and minor groove positioning with RNA targets.

4. Pyrene-functionalized LNA

4.1 Biophysical characteristics of LNA

Locked nucleic acid (LNA) was independently developed in the end of the 1990's by the Wengel[45] and Imanishi[46] laboratories (Fig. 3). The oxymethylene bridge spanning the C2′- and C4′-positions efficiently locks the furanose ring in a C3′-*endo* conformation similar to the conformations of ribonucleotides in RNA duplexes.[47] Moreover, the biyclic LNA skeleton restricts the glycosidic torsion angle due to a steric clash between H6(pyrimidine)/H8(purine) and the pseudoaxial H3', which is exacerbated by the large puckering amplitude of LNA nucleotides (Fig. 3).[48] Incorporation of LNA monomers into ONs results in pre-organization of neighboring nucleotides toward increased *N*-type sugar conformation character, both in single stranded ONs[47,49] and corresponding duplexes with complementary DNA/RNA.[47,50] The limited internal flexibility of LNA nucleotides restricts conformational interconversion of adjacent nucleotide residues as they are mechanically coupled, whereby duplex dynamics are damped.[51] As a result, LNA-modified ONs display very high thermal affinity toward single stranded DNA/RNA targets (ΔT_m/mod up to +10 °C) and high target specificity (i.e., mismatch discrimination). LNA has, accordingly, been extensively explored as a fundamental research tool for modulation of gene expression via the antisense approach and evaluated as a RNA-targeting drug candidate against diseases of genetic origin.[52]

One of the LNA diastereoisomers, i.e., α-L-LNA (Fig. 3) shares many of the desirable hybridization properties of LNA despite its `unnatural' configuration at the C2'-, C3'- and C4'-positions.[53] Unlike LNA, which is considered an RNA mimic, α-L-LNA is considered a DNA mimic since duplexes between DNA/α-L-LNA-mixmers and DNA or RNA complements adopt geometries that globally resemble unmodified duplexes.[54,55] It follows that α-L-LNA also is as an interesting antisense building block.[56] For additional background on the LNA technology, we refer to the following reviews.[57–58]

In light of the beneficial hybridization properties and conformational rigidity of LNA, α-L-LNA and the corresponding 2'-amino analogs,[59–60] the Wengel and Hrdlicka laboratories set out to develop pyrene-functionalized LNAs to study the fundamental properties of duplexes composed of PFOs that offer a high degree of positional control of the pyrene moiety (Fig. 4).

4.2 LNA monomers with nucleobase surrogates

Wengel and coworkers have developed three different LNA monomers where a pyrene has replaced the nucleobase moiety, i.e., LNA *C*-glycoside **29**,[61] α-L-LNA *C*-glycoside **30**,[62] and LNA aminomethyl *C*-glycoside monomer **31** (Fig. 4).[63] Interestingly, the affinity-enhancing effect of the LNA skeletons is fully compromised as evidenced by the extensive destabilization of singly modified DNA duplexes (ΔT_m down to −11 °C). These probes display similar universal base behavior as the structurally simpler monomer **1** (Fig. 2).

4.3 Nucleobase-modified LNA monomers

Hrdlicka and coworkers developed a series of C5-functionalized LNA and α-L-LNA pyrimidines based on the hypothesis that the conformationally restricted sugar ring and restricted glycosidic torsion angle would reduce the available conformational space for C5-substituents in the major groove relative to DNA analogs. C5-functionalized LNA carrying non-aromatic moieties are tolerated extraordinarily well in nucleic acid duplexes (ΔT_m/mod up to + 13 ° C).[64] Interestingly, incorporation of 5-[3-(1-pyrenecarboxamido)propynyl]-functionalized LNA and α-L-LNA monomers **32** and **35** into DNA duplexes (Fig. 4) results in similar decreases in DNA duplex thermostability (ΔT_m/mod = −5 to −2 °C) as the corresponding 2'-deoxyuridine analog **4** (Fig. 2).[11] Similar trends have been observed for C5-triazole-linked pyrene-functionalized LNA monomers **33**[65] and **34**[65] (Fig. 4) relative to their corresponding 2'-deoxyuridine analogs (for **6**: ΔT_m/mod = −14 to −4 °C, for **8**: ΔT_m/mod = −7 to +2 °C).[21] Although the stabilizing effects of the parent LNA and α-L-LNA skeletons are largely compromised by these C5-substituents, fluorescence emission spectra suggest that high positional control of the fluorophore is realized (*vide infra*).[11]

4.4 N2'-Functionalized 2'-amino-LNA & 2'-amino-α-L-LNA

N2'-functionalized 2'-amino-LNA[66] and 2'-amino-α-L-LNA[67] were developed by Wengel, Hrdlicka and coworkers based on the hypothesis that a N2'-substituent attached via a short linker would be positioned more precisely within duplexes than with more flexible monomers. Most N2'-functionalized 2'-amino-LNA display similar thermal affinities toward complementary DNA/RNA targets as the corresponding parent LNA.[66] ONs modifed with 2'-*N*-(pyren-1-yl)carbonyl-2'-amino-LNA monomer **37** also follow this trend, while ONs modified with the slightly more flexible 2'-*N*-(pyren-1-yl)methyl-2'amino-LNA monomer **36** display more modest thermal affinities toward complementary DNA/RNA (Fig. 4). Fluorescence emission spectra (*vide infra*) and molecular modeling studies suggest that the N2'-substituent predominantly is located in the minor groove (Fig. 5).

2'-Amino-α-L-LNA carrying non-aromatic moieties at the N2'-position display dramatically decreased thermal affinity toward DNA/RNA targets (e.g., ΔT_m/mod down to −16.5 °C for a N2'-acetyl group).[67] In contrast, exceptional increases in duplex thermostability are observed for ONs modified with pyrene-functionalized monomers **38**, **39** and **40** (Fig. 4). DNA:DNA duplexes are significantly more stabilized than DNA:RNA duplexes (vs DNA: ΔT_m/mod = 6–15, 10–19 and 10–16 °C, respectively; vs RNA: ΔT_m/mod = −1 to +7, 4–11 and 6–12 °C, respectively).[67] The extensive DNA selectivity, along with hybridization-induced bathochromic shifts of pyrene absorption maxima, increased circular dichroism signal intensity in the pyrene region, and molecular modeling studies, suggest pyrene intercalation in the duplex core. Closer scrutiny of the molecular structure reveals that the 2-

oxo-5-azabicyclo[2.2.1]heptane skeleton of monomers **38–40** is locking the attachment points of the nucleobase and the pyrene moiety (i.e., C1' and N2') relative to each other. This, along with the short linkers connecting the pyrene units to the bicyclic skeleton, most likely, preorganizes the pyrene moieties to intercalate in the 3'-direction (Fig. 6).

5. Generation of pyrene arrays on nucleic acids

Nucleic acids have received considerable attention due to their potential as building blocks in bottom-up nanotechnology due to: a) their predictable and programmable self-assembly that is governed by Watson-Crick base pairing rules; b) their well-defined and naturally nanometer-sized dimensions; c) their straightforward synthesis and; d) the availability of experimental techniques for additional structural manipulation of nucleic acids (e.g., ligation, digestion, PCR amplification). A remarkable range of DNA-based structures such as nanowires, lattices and octahedrons have been reported.[68] Periodic organization of matter (e.g., nanoparticles and proteins) on two-dimensional DNA arrays is one of many promising applications of bottom-up DNA nanotechnology. The use of nucleic acids as supramolecular scaffolds for arrangement of chromophores has lately received considerable interest due to the prospect of developing DNA-based light harvesting complexes.[3,69,70] Pyrene arrays have been studied as a first step toward this end.

5.1 Pyrene arrays in the minor groove

Nakamura, Yamana and coworkers hybridized 2'-*O*-methyl RNA strands that are sequentially modified with 2'-*O*-(pyren-1-yl)methyluridine **21** monomers to RNA complements (Fig. 7).[71] The intense excimer emission along with data from UV-vis spectroscopy, circular dichroism and molecular modeling studies, provides indirect evidence for formation of pyrene arrays in the minor groove (Fig. 7).[71]

Wengel, Hrdlicka and coworkers used two complementary ONs modified with 2'-*N*-(pyren-1-yl)methyl-2'amino-LNA monomer **36** to form DNA duplexes featuring interstrand pyrene arrays in the minor groove (Fig. 8).[72] Thus, positioning of monomers **36** i n "−1 interstrand zipper arrangements" results in extensive duplex stabilization and intense excimer formation signifying strong stacking arrangements of pyrene moieties. The increased duplex thermostability is particularly noteworthy considering that isolated **36** monomers only have minor effect on thermostability (Fig. 8).[72] More brightly fluorescent analogs of this excimer-forming communication system, based on 2'-amino-LNA monomers that are N2-functionalized with 1-, 2- and 4-(phenylethynyl)pyrenes, have been developed recently.[73] Incorporation of these excimer-forming switches at strategic positions has been utilized to signal stepwise self-assembly of higher order nucleic acid structures (Fig. 8).[74]

Nakamura, Yamana and coworkers subsequently generated interstrand pyrene-zipper arrays in the minor groove using RNA duplexes modified with 2'-*O*-(pyren-1-yl)methyl uridine/adenosine pairs (i.e., 0-interstrand zippers) positioned as next-nearest neighbors.[75] Array formation is supported by intense excimer emission and molecular modeling studies. While formation of the pyrene array counteracts the negative impact on RNA duplex thermostability by 2'-*O*-(pyren-1-yl)methyl nucleotides, the resulting duplexes are still less stable than unmodified RNA duplexes.[75] The extraordinary duplex thermostability, directional preference and robustness of the 2'-*N*-(pyren-1-yl)methyl-2'amino-LNA communication system, underscores the potential advantages of pyrenefunctionalized LNA.[72]

5.2 Pyrene arrays in the major groove

Positioning of pyrenes in the major groove of nucleic acid duplexes was first suggested by Korshun and coworkers who utilized DNA duplexes modified with `+2 interstrand zipper arrangements' of *arabino*-configured 2'-carbamate monomer **18** (Fig. 2), resulting in the formation of excimers.[40]

Wagenknecht and coworkers observed a) strong exciton coupling of pyrene signals in the circular dichroism spectra and b) strongly increased and blue-shifted fluorescence emission (λ_{em} ~ 445 nm) upon hybridization of ONs containing five sequential incorporations of 5-(pyren-1-yl)-2'-deoxyuridine monomer **2** (Fig. 2) with complementary DNA, which indicates formation of an electronically coupled pyrene array in the major groove.[76] Interestingly, hybridization with DNA strands containing two or more mismatched nucleotides opposite of the modified region, results in less intense fluorescence emission, suggesting that the presence of mismatched base pairs perturbs the electronically coupled organization of pyrenes.[76] Similar observations have been made with the corresponding 5-(1-ethynylpyrenyl)-2'-deoxyuridine monomer **3** (Fig. 2).[77]

5.3 Pyrene arrays in the duplex core

The nucleic acid duplex core can be engineered to generate metal ion arrays.[78] Similarly, pyrene arrays can be formed inside duplex cores due to the comparable π-stacking area of pyrene moieties and Watson-Crick base pairs. Kool and coworkers demonstrated that DNA duplexes containing `base pairs' between *C*-glycoside **1** and abasic sites Φ display similar thermostability as reference duplexes with native A:T pairs (Fig. 2).[20] However, duplex integrity is lost if more than two out of ten regular base pairs are replaced by **1**:Φ pairs.[20] Similar results have been observed using LNA aminomethyl *C*-glycoside monomer **31**.[63]

Hrdlicka, Wengel and coworkers studied hybridization properties of ONs modified with 5'-(**Y**Φ)-units, i.e., where a 2′-*N*-(pyren-1-yl)acetyl-2′-amino-α-L-LNA monomer **40** (= **Y**) is flanked by an abasic site Φ on the 3′-side.[79] These ONs display extraordinary thermal affinity toward DNA strands containing abasic sites in +1 interstrand positions (Fig. 9). Thus, a 13-mer DNA duplex containing four of these 5'-(**Y**Φ):3'-(**A**Φ)-units separated by one base pair, exhibits a thermal denaturation temperature of ~60 °C. In contrast, the corresponding 13-mer reference duplex where 5'-(**Y**Φ):3'-(**A**Φ)-units are replaced by 5'-(TA):3'-(AT) base pairs has a T_m of 35 °C. Molecular modeling studies strongly suggest that the pyrene moiety of N2'-functionalized 2'-amino-α-L-LNA monomer **40** is located in the duplex core void formed by the Φ:Φ pair and partakes in efficient π-π stacking with neighboring base pairs (Fig. 9).[79]

Häner and coworkers have recently developed so-called oligopyrenotides, i.e.,. `duplexes' composed of achiral phosphodiester-linked pyrene building blocks and a single chiral 1,2-diaminocyclohexane, which feature a continuous pyrene array in the core. This highlights the possibility of creating purely artificial self-assembling structures and demonstrates the potential of pyrene moieties as building blocks in nanotechnology.[80]

The use of nucleic acids as supramolecular scaffolds to arrange fluorophores in arrays can be used to force two or more fluorophores to interact in the excited state to form red-shifted excimers (between identical fluorophores) or exciplexes (between different fluorophores).[81] Kool and coworkers studied all 4096 combinations (8^4 = 4096) of a tetramer that is modified at every position with any of eight building blocks (seven different *C*-glycosides or an abasic site). This resulted in the isolation of tetramers with very different emission characteristics (λ_{max} = 376–633 nm) despite using identical excitation conditions (λ_{em} = 340–380 nm).[82]

6. Diagnostic applications of PFOs

Reliable detection of specific nucleic acid sequences is an integral component of a wide range of applications including quantification of DNA/RNA in real-time PCR,[83] detection of acceptor sites for antisense oligonucleotides,[84] visualization of RNA trafficking in cells,[85] detection of SNPs,[86] and pathogen detection.[87] Development of fluorophore-modified ONs,[88] and PFOs in particular, has received major attention over the past decade. Pyrene-functionalized monomers are used as components of a) hybridization probes, b) base discriminating fluorescent probes, c) excimer-forming probes, and d) quencher-free molecular beacons.

6.1 Hybridization probes

Hybridization probes are designed to display a) low levels of fluorescence emission in the single-stranded state, typically through quenching interactions between pyrene and nucleobase moieties,[9] and b) high levels of fluorescence emission in the double-stranded state by placing the pyrene moiety in a non-quenching environment (Fig. 10).

Yamana, Murakami and coworkers discovered that hybridization between RNA probes modified with 2'-*O*-(pyren-1-yl)methyluridine monomer **21** (Fig. 2) and RNA targets results in pronounced increases in fluorescence intensity (10–30-fold) to give duplexes with emission quantum yields up to 24%.[36] Much smaller increases are observed upon hybridization with DNA targets,[36] or if corresponding DNA probes are hybridized to DNA/RNA targets.[35] This reflects the fact that intercalation of the pyrene moiety into the quenching base stack is a major binding mode in DNA:DNA and DNA:RNA, but not RNA:RNA duplexes.[37] These data demonstrate how functional control is closely linked with positional control of the pyrene moiety. 2'-*O*-methyl-RNA probes modified with monomer **21** display extraordinary increases in fluorescence intensity upon hybridization with RNA (up to ~300-fold) but only if flanked by a 3'-cytosine or guanine moiety, which limits the generality of these probes. These neighboring bases are most likely needed to ensure sufficient quenching of the single stranded probe.[84] A hexitol nucleic acid (HNA) analog of monomer **21**, i.e., monomer **41** (Fig. 11), has recently been incorporated into HNA backbones. However, only very modest changes in fluorescence intensity were observed upon hybridization with RNA targets.[89]

Hrdlicka and coworkers have developed hybridization probes based on ONs modified with a single pyrene-functionalized triazole-linked 2'-deoxyuridine monomer **8** (Fig. 2). Hybridization with complementary DNA or RNA targets results in very large increases in fluorescence emission at λ_{em} = 382 nm (9- to 23-fold), except when monomer **8** is flanked by thymine moieties. Emission quantum yields up to 16% were observed.[21]

In a different study, Hrdlicka, Wengel and coworkers discovered that DNA strands modified with 2'-*N*-(pyren-1-yl)carbonyl-2'-amino-LNA monomer **37** display large increases in fluorescence intensity upon hybridization with complementary DNA and RNA (between 2.5- and 69-fold).[90] To achieve such increases, two or more non-sequential **37** monomers must be incorporated into ONs since a) this lowers the fluorescence intensity of single stranded probes by facilitating quenching interactions between pyrene and/or nucleobase moieties, and b) each incorporation results in near-additive increases in fluorescence intensity.[90] Duplexes between appropriately designed probes and DNA/RNA targets are highly thermostable and brightly fluorescent with emission quantum yields between 28–99% (Table 1). Equivalent RNA or 2'-*O*-methyl-RNA backbone-based probes lead to even larger hybridization-induced increases in fluorescence intensity due to more efficient fluorescence quenching of the single stranded probes and higher duplex quantum yields.[91] Phosphorothioate DNA (PS-DNA) based probes display similar characteristics as the parent

DNA probes, whereas single stranded LNA backbone-based probes display high quantum yields even when they are doubly modified. This presumably reflects pre-organization of the single-stranded LNA in a duplex-like conformation. The observed duplex quantum yields with these `Glowing LNA' are two- to four-fold higher than for state-of-the-art PFOs composed of 2'-*O*-(pyren-1-yl)methyluridine **21**[36] or C4-pyrene-functionalized monomer **27**[33] (Fig. 2), which is an unlocked variant of monomer **37**. Moreover, Glowing LNA are a) much less sensitive to the nature of flanking nucleotides than other PFO-based hybridization probes,[90,92] and b) equally suitable for detection of DNA and RNA targets.[90–92] These desirable optical characteristics are hypothesized to be a consequence of the conformationally locked bicyclic skeleton and the short amide linkage of monomer **37** working in concert to firmly position the pyrene moiety in the non-quenching minor groove (Fig. 5).[90]

Several Glowing LNA analogs have been subsequently studied. Wengel and coworkers changed the fluorophore from (pyren-1-yl)carbonyl to various (phenylethynyl)pyrene moieties which generally results in red-shifted absorption and fluorescence emission. High quantum yields are observed for some of these analogs but it is currently unclear if they follow similar design guidelines and are as general as the parent Glowing LNA.[19,73] Chattopadhyaya and coworkers attached the (pyren-1-yl)carbonyl moiety on two other conformationally restricted nucleotides, i.e., azetidine and aza-ENA (ethylene nucleic acid) thymine monomers **42** and **43**, respectively (Fig. 11).[93] DNA strands that are singly modified with monomer **42** display strongly reduced thermal affinity toward RNA targets and duplex quantum yields that vary considerably with the sequence context (Φ_F = 0.06–0.73, lower with 3'-flanking G). Hybridization to complementary RNA only results in modestly increased quantum yields; however, it is possible to observe large hybridization-induced increases at λ_{ex} = 378 nm since hybridization is accompanied with a marked blue-shift in fluorescence emission due to destacking of the pyrene and nucleobase moieties. ONs that are singly modified with monomer **43** seem to display smaller hybridization-induced increases in fluorescence intensity and duplex quantum yields (9–47%) than the parent Glowing LNA but direct comparison is complicated by the use of different sequence contexts.[93] Even the conservative change from a (pyren-1-yl)carbonyl moiety to a slightly more flexible (pyren-1-yl)methyl moiety (i.e., monomer **36**, Fig. 4) results in markedly less intense fluorescence emission.[72] Collectively these examples indicate the importance of precise positioning of the pyrene moiety to achieve the desired function.

6.2 Base discriminating fluorescent probes

ONs modified with base discriminating fluorescent (BDF) monomers generate different levels of fluorescence emission based on the nature of the nucleotide opposite of the modification.[94–95] Most BDF probes that are based on pyrene-functionalized monomers rely on a simple principle - the pyrene moiety is a) positioned in a non-quenching groove upon hybridization with complementary targets while, b) being intercalated up on hybridization with non-complementary targets, leading to quenching of fluorescence by flanking nucleobases (typically cytosine or guanine, Fig. 12). Unlike hybridization probes, BDF probes can discriminate between complementary and mismatched targets at non-stringent conditions where mismatched duplexes are formed. Accordingly, BDF probes are well-suited to discriminate SNPs, which are the most frequently occurring genetic variation in the human genome (>9 million SNPs) and important biomedical markers.[96]

The use of ONs modified with C5-pyrene-functionalized pyrimidine monomers has proven to be a robust approach toward successful BDF probe design. Among the numerous linker variants that have been studied,[21,26,97–99] the C5-[3-(1-pyrenecarboxamido)propynyl]-functionalized 2'-deoxyuridine monomer **4** emerges as a particularly interesting BDF

monomer (Fig. 2), which has been used to discriminate SNP sites in human breast cancer 1 (BRCA 1) gene.[26,100] As discussed earlier, molecular modeling studies and fluorescence emission spectra suggest that the nucleobase of monomer **4** adopts an *anti* conformation (Watson-Crick base pairing orientation) upon hybridization with complementary DNA to position the pyrene in the major groove, while adopting a *syn* conformation with mismatched DNA leading to pyrene intercalation (Fig. 12).[26]

Hrdlicka and coworkers recently developed the corresponding LNA and α-L-LNA analogs **32** and **35** (Fig. 4) based on the hypothesis that indirect restriction of the glycosidic torsion angle (see section 4.1 and Fig. 3) would result in higher positional control of the polarity-sensitive C5-fluorophore and potentially enhance SNP discrimination.[11] A systematic comparison of the DNA, LNA and α-L-LNA monomers revealed the following. First, ONs modified with DNA monomer **4** (i.e., parent probes) require flanking C/G-moieties for efficient fluorescent mismatch discrimination. Second, ONs modified with LNA analog **32** display higher quantum yields (Φ_F = 0.44–0.67) and pyrene extinction coefficients upon hybridization with complementary DNA than parent probes; probes where **32** is flanked by C/G-moieties display more efficient fluorescent discrimination of mismatched targets (Fig. 13). Third, ONs modified with α-L-LNA analog **35** also display higher quantum yields (Φ_F = 0.50–0.80) upon hybridization with complementary DNA; probes where **35** is flanked by A/T-moieties display improved fluorescent discrimination of mismatched targets compared to the parent probes.[11] The higher duplex quantum yields observed with ONs modified with monomers **32** and **35**, most likely, reflect higher positional control of the fluorophore in the major groove.

C7-deaza- and C8-pyrene-functionalized 2'-deoxyadenosines **16** and **14** (Fig. 2) also display BDF characteristics. ONs modified with monomer **16** display low emission upon hybridization with complementary DNA and higher emission with singly mismatched targets.[30] Intriguingly, the opposite trends are observed for equivalent probes modified with monomer **14**.[28] The mechanism and binding modes of these flexible probes are not yet understood. C4-pyrene-functionalized monomer **27**[33] is a rare example of a BDF-monomer where the pyrene moiety is linked to the sugar moiety. The pyrene moiety is presumably located in the minor groove upon hybridization with complementary DNA (high fluorescence), while intercalating upon hybridization with mismatched DNA targets (low fluorescence).[33]

In an interesting extension of the BDF probe concept, C5-[3-(1-pyrenecarboxamido)propynyl]-functionalized 2'-deoxyuridine monomer **4** was incorporated into a DNA strand and positioned 2–5 nt from a flexible 5'-terminal fluorescein moiety. Duplexes with complementary DNA display Fluorescence Resonance Energy Transfer (FRET) from pyrene to fluorescein (λ_{ex}= 340 nm, λ_{em}= 520 nm). In contrast, less efficient FRET is observed upon hybridization to singly mismatched DNA targets, presumably due to intercalation and quenching of the pyrene fluorophore.[101]

6.3 Excimer-forming probes

The large Stoke's shift (~120 nm) of pyrene-pyrene excimers render them attractive for nucleic acid diagnostics as this may reduce background fluorescence from unbound probes. As mentioned previously, duplexes between RNA targets and 2'-*O*-methyl RNA probes modified with two sequential 2'-*O*-(pyren-1-yl)methyluridine **21** monomers display excimer emission due to pyrene-pyrene interactions in the minor groove (Fig. 7). Duplexes with mismatched base pairs proximal to the modified region only display very low levels of excimer emission.[102] These probes do not allow discrimination of mismatched DNA targets since the intercalative binding mode of the pyrene moiety in matched 2'-*O*-methyl-

RNA:DNA heteroduplexes prevents excimer formation.[93] ONs with sequential modifications of 2'-*N*-(pyren-1-ylmethyl)-2'-amino-LNA monomer **36** address this point presumably since the pyrene moieties are forced into the minor groove (*vide infra*).[103]

Dual probes[104] based on end-labelled PFOs are another class of excimer-forming probes.[105] Two short probes are assembled into a ternary complex upon binding with a complementary target, which generates an excimer signal. Monomer fluorescence is predominantly observed in absence of target (Fig. 14).[104–105] Wengel and coworkers evaluated extensively LNA-modified ONs end-labelled with 2'-*N*-(pyren-1-ylmethyl)-2'-amino-LNA monomer **36** in SNP dual probe assays (Fig. 14).[103] As expected, binding with complementary 17-mer DNA or RNA targets results in excimer emission due to productive pyrene-pyrene interactions in the ternary complex. In contrast, addition of singly mismatched DNA or RNA targets leads to significantly lower excimer emission (Fig. 14). Thermal denaturation temperatures of matched/mismatched complexes suggest that the decreased excimer intensity is a result of a) mismatch-induced local structural perturbation of the ternary complex whereby pyrene moieties adopt unsuitable conformations for excimer formation (positions 8–11, Fig. 14), or b) lack of ternary complex formation due to thermal mismatch discrimination, which is particularly efficient due to the short probe length and high LNA content (positions 2–7, Fig. 14).[103] The LNA-based dual probe platform appears to result in more pronounced SNP-discrimination than other dual probes based on more flexible monomers, but direct comparison is complicated by the use of different nucleic acid targets.[105–106] The covalently linked 17-mer analog of the 8- and 9-mer dual probes also displays excimer emission upon hybridization with complementary DNA and decreased excimer emission with mismatched DNA targets, but optical discrimination is only efficient in a narrower region (positions 7–10) through local structural pertubation.[103] This underlines the advantage of the dual probe approach, i.e., the combination of local structural pertubation and thermal mismatch discrimination to achieve optical discrimination of SNP-containing targets.

Two recent developments within the dual probe technology merit special mention. First, excimer-forming PFO-based dual probes have been coupled with time-resolved fluorescence spectroscopy to discriminate between short-lived background fluorescence and pyrene excimers with long fluorescence lifetimes (> 40 ns); this facilitated SNP-analysis of biological samples.[107] Secondly, dual probes based on hybridization-induced formation of exciplexes between a pyrene- and a *N*,*N*-dialkylnapthalene-labelled probe have been developed.[106] The main advantage of this approach is the potential for multiplexed DNA detection as different exciplex partners with unique emission characteristics can be designed. A potential limitation of this detection platform, however, is that trifluoroethanol is a necessary additive since water quenches exciplex fluorescence emission.[108]

Another approach that employs pyrene-pyrene excimer fluorescence and which does not require stringent control of experimental temperatures for SNP-detection, is based on ONs with two incorporations of 2′-*N*-(pyren-1-yl)acetyl-2′-amino-α-L-LNA monomer **40** as next-nearest neighbors (Fig. 15).[109] Duplexes with complementary DNA/RNA targets predominantly display pyrene monomer fluorescence, whereas DNA/RNA duplexes with mismatched base pairs proximal to the modified region (positions 4–7, Fig. 15) display significantly increased excimer emission (2- to 11-fold increase at λ_{em} = 480 nm). As previously discussed, the pyrene moiety of monomer **40** is forced into the core of matched duplexes resulting in extensive duplex stabilization and monomer fluorescence. Mismatched duplexes appear to induce a more flexible geometry, which allows the pyrene moieties to adopt extrahelical orientations suitable for formation of pyrene-pyrene excimers.[109] A related platform has been developed based on non-nucleosidic pyrenefunctionalized “Intercalating Nucleic Acid” (INA) monomers (Fig. 19). SNP discrimination appears to be less efficient but comparative studies have not been performed.[110]

6.4 Quencher-free molecular beacons

In the original molecular beacon (MB) design, single stranded probes adopting a stem-loop structure are end-functionalized with a fluorophore-quencher pair.[111] In the absence of targets, the fluorophore and quencher are in close proximity of each other leading to low fluorescence emission levels. Binding to a single stranded target that is complementary to the loop region results in MB opening, spatial separation of the fluorophore-quencher pair, and increased fluorescence emission (Fig. 16A). A key advantage of MBs over linear probes is that they display improved thermal discrimination of mismatched targets, which reduces the risk of false positives.[111] Numerous *quencher-free MBs*, including several that are based on PFOs, have recently been developed based on prospects of simpler design, lower costs, and potential for secondary modification via end-functionalization.[112]

Hrdlicka and co-workers designed quencher-free MBs based on 29-mer DNA or 2'-*O*-methyl RNA strands, which are modified with four separated incorporations of Glowing LNA monomer **37** in the 15-mer loop region (Fig. 16B, shown for singly modified MB).[91] Hybridization with complementary DNA/RNA targets results in 3- to 9-fold increases in fluorescence intensity and formation of brightly fluorescent duplexes (Φ_F = 0.45–0.85). These changes arise, in all probability, due to translocation of the pyrene moieties from a single-stranded environment where quenching interactions with nucleobases occur to the non-quenching minor groove. Glowing LNA beacons display excellent thermal discrimination of singly mismatched DNA/RNA targets and high biostability (> 48h), which enabled their use for detection of specific mRNA in murine 3T3-L1 cell cultures.[91]

In a different approach, Kim and coworkers incorporated 8-(1-ethynylpyrenyl)-2'-deoxyadenosine monomer **11** into MBs as a 5'-dangling residue which results in a) efficient π–stacking with the terminal base pair, and b) quenching of fluorescence through photoinduced electron transfer which depends on the nature of the 5'-flanking nucleotide in the following manner: C>G>T>A (Fig. 16C).[10] In related approaches,[113–114] Saito and coworkers, e.g., introduced a pyrene-labeled pyrrolocytidine monomer in the middle of a MB stem leading to quenching of fluorescence through interactions with the pairing guanine moiety.[114] Binding of these MBs to complementary DNA results in a) MB opening, b) localization of the pyrene moiety in a single stranded region, and c) dequenching due to reduced nucleobase interactions.[10,114]

In yet another approach, incorporation of two flexible non-nucleosidic pyrene units at the termini of 29-mer DNA-based MBs leads to efficient pyrene-pyrene-stacking and formation of excimer fluorescence (Fig. 16D).[115] Similarly, incorporation of two 8-(1-ethynylpyrenyl)-2'-deoxyadenosine **11** monomers opposite of each other within the stem of a 27-mer DNA-based MB, leads to excimer emission in the closed state presumably since nucleobases adopt *syn* conformations.[116] Hybridization with complementary DNA results in MB opening, separation of the pyrene moieties, and a marked increase in the monomer/excimer intensity ratio (Fig. 17). Virtually no change in the monomer/excimer intensity ratio is observed upon hybridization with singly mismatched DNA targets, which underlines the high thermal mismatch discrimination of MBs.[115–116]

The opposite principle has been used in MBs with two proximal incorporations of flexible C8-pyrene functionalized monomer **10** in one stem arm. In the absence of target strands, the pyrene moieties predominantly display monomer fluorescence. Upon binding with complementary targets, the beacon opens up, the stem becomes single-stranded, and the pyrene moieties interact with each other to generate excimer fluorescence.[117] Similar observations were made with MBs modified with 1–4 flexible pyrene moieties at the 5'-end and a 3'-DABCYL quencher.[118]

Wagenknecht and coworkers incorporated 5-(1-ethynylpyrenyl)-2'-deoxyuridine monomer **3** into the stem of MBs in close proximity of a 2'-deoxyuridine modified at the C5-position with a `Nile Red' fluorophore. In the closed state, efficient FRET from pyrene to Nile Red results in fluorescence emission at 435 nm and 660 nm (pyrene and Nile Red, respectively). Opening of the MB upon DNA target binding, results in separation of the FRET donor-acceptor pair and an increase in the I_{435}/I_{660} ratio enabling ratiometric DNA detection.[119]

6.5 Miscellaneous diagnostic applications of PFOs

Pyrene-functionalized monomers have been used to study formation of alternative nucleic acid structures.[98,120–121] Silverman and coworkers systematically modified the P4–P6 domain of Tetrahymena group I intron with N2'-pyrene-functionalized 2'-amino-DNA monomers to study RNA folding. Mg^{2+}-induced formation of tertiary structures results in increases in fluorescence emission when long-linked monomers are used, presumably since the pyrene moiety is translocated from a stacking to a non-stacking environment.[120]

Kim and coworkers attached 8-(1-ethynylpyrenyl)-2'-deoxyadenosine monomer **11** as a dangling residue of G-rich ONs.[121] In the single stranded state these ONs exhibit fluorescence emission at λ_{em} = 451 nm; addition of potassium ions results in a) G-quadruplex formation, b) stacking between pyrene and terminal guanosines, and c) exciplex formation. As a result, red-shifted fluorescence emission is observed (λ_{em} = 485 nm, Fig. 18).[121] This is particularly interesting given the recent focus on G-quadruplexes as materials for bottom-up fabrication of nanomaterials.[122]

Okamoto, Saito and coworkers used a CG-alternating ON modified with 8-(1-ethynylpyrenyl)-2'-deoxyguanosine monomer **12** and C5-[3-(1-pyrenecarboxamido)propynyl]-functionalized 2'-deoxycytosine (i.e., the C-analog of monomer **4**, Fig. 2), to monitor salt-induced transitions from a right-handed *B*-type to left-handed *Z*-type DNA-duplex. Presumably, monomers **4** and **12** adopt *anti*- and *syn*-conformations, respectively, which positions the pyrene moieties far apart at low salt concentrations (*B*-type) while leading to π-stacking and excimer formation at high salt concentrations (*Z*-type).[98]

PFOs have also been utilized to study protein-nucleic acid interactions. Seitz, Weinhold and coworkers reported that DNA duplexes modified with pyrene glycoside **1** (Fig. 2) bind ~400 times more strongly to adenine-specific DNA methyltransferase (MTase) M·*Taq*I than corresponding unmodified DNA duplexes. The DNA methylations catalyzed by this enzyme commence by flipping the target nucleotide to an extrahelical position. The resulting void is more efficiently stabilized by the pyrene moiety of monomer **1** than by natural nucleobases.[123] Stivers and coworkers used DNA duplexes modified with monomer **1** to study the mechanism of uracil DNA glycosylase, i.e., a DNA repair enzyme which also proceeds via base-flipping of a nucleotide.[124]

Kim and coworkers incorporated monomer **3** (Fig. 2) into the U25 bulge region of HIV TAR RNA which undergoes a substantial conformational change upon binding with Tat-protein mimics. Binding leads to reduced interactions between the pyrene moiety and adjacent base pairs and dequenching of fluorescence emission. Such probes may, accordingly, be useful to identify RNA-binding entities.[125]

7. Targeting of double stranded DNA using PFOs

Chemically modified ONs are widely utilized to modulate gene expression, which has enabled gene function studies and led to development of drug candidates against diseases of genetic origin. The vast majority of these efforts have focused on targeting of RNA.[126]

Development of probes for sequence-specific targeting of double stranded DNA (dsDNA) has received far less attention, despite the prospect of powerful tools for modulation of gene expression, gene manipulation, and detection of dsDNA in living cells.[127–128] From a chemical perspective, dsDNA is a significantly more complex target than single stranded DNA/RNA since the Watson-Crick hydrogen-bonding faces are buried in the duplex core. This leaves few molecular `handles' for sequence-specific recognition of dsDNA. Probes targeting dsDNA in biological contexts face the additional challenge of compacted and protein-associated chromosomal DNA. Triplex forming oligonucleotides (TFOs), which bind in the major groove through relatively weak Hoogsteen base pairs, are the most extensively explored dsDNA-targeting technology. Limitations of TFOs include: a) requirement for long homopurine target regions (>15 nt) to ensure sufficient binding affinity/specificity; b) the need for slightly acidic pH to ensure cytosine protonation which is required for Hoogsteen base pairs between TC-motif TFOs and dsDNA; and c) undeisred formation of secondary structures by G-rich TFOs at physiological potassium ion concentrations, which affects dsDNA binding capabilities. For further discussion of the TFO-technology, the Reader is directed to the review by Arimondo and coworkers.[129] The limitations of the TFO-technology have spurred a search for alternative dsDNA-targeting strategies including minor groove binding polyamides, peptide nucleic acids (PNAs), pseudo-complementary PNA (pc-PNA), and other approaches which have been recently reviewed by Concordet, Giovannangeli and coworkers and that are not further discussed herein.[130]

PFOs have been explored for dsDNA-targeting applications. Pedersen, Filichev and coworkers introduced non-nucleosidic “Twisted Intercalating Nucleic Acid” (TINA) monomer **45** as bulges in TC-motif TFOs (Fig. 19).[131] Increases in triplex thermostability are observed that vary with TFO length, pH and the number, position, and distance between modifications (Δ_{Tm}/mod 0–20 °C).131–132 Molecular modeling studies suggest that the pyrene moieties are situated in the Watson-Crick-paired dsDNA part of the triplex, while the phenyl moiety stacks with the nucleobases of the TFO.[133] The low triplex thermostability at physiological pH and TFO-based sequence limitations remain challenges that need to be addressed.

Hrdlicka and coworkers have proposed a radically different approach for dsDNA-targeting which utilizes *Invader LNA probes* (Fig. 20), i.e., DNA duplexes modified with one or more +1 interstrand zipper arrangements of 2'-*N*-(pyren-1-yl)methyl-2'-amino-α-L-LNA thymine monomer **38** (Fig. 4).[134–135] Invader LNA display low probe duplex thermostability, which is related to the “nearest neighbor exclusion principle”[5]; the 2-oxo-5-azabicyclo[2.2.1]heptane skeleton presumably forces the pyrene moieties of +1 zipper-positioned **38** monomers to intercalate into the same region as demonstrated by excimer formation. Due to constraints in local helix expandability, this `energetic hotspot' leads to partial duplex unwinding and decreased thermostability.[134–135] Other interstrand zipper arrangments of monomer **38** result in much higher duplex thermostability, which underlines the importance of positional control to achieve functional control.[134–135] Both strands of the Invader LNA probes display very high thermal affinity toward complementary DNA (ΔT_m/mod up to +15 °C).[67] These large differences in duplex thermostability have been exploited to enable spontaneous recognition of isosequential, mixed-sequence dsDNA targets under non-denaturing conditions (Fig. 20).[134–135] The recognition process is conveniently monitored in-real time by the decrease in excimer emission as the pyrene moieties are forced apart (Fig. 20), or by taking advantage of the different electrophoretic mobilities of Invader LNA, dsDNA targets and probe:target-duplexes.[135] Thus, addition of a pre-annealed 13-mer Invader LNA to an equimolar quantity of the isosequential dsDNA target at 110 mM NaCl, pH 7 and low incubation temperatures, results in 50% recognition within ~40 min; shorter targets, higher incubation temperatures and/or the use of Invader LNA with more than one

energetic hotspot, accelerate molecular recognition. It is particularly noteworthy that dsDNA-recognition even occurs in buffers of very high ionic strengh (710 mM NaCl, pH 7, $t_{50\%}$ ~125 min). When Invader LNA are mixed with dsDNA where one base pair is exchanged relative to Invader LNA (i.e., non-isosequential dsDNA targets), much slower and less pronounced decay of the excimer signal is observed, underlining that the recognition process is sequence-specific. The recognition mechanism is not fully understood, but may involve partial melting of dsDNA targets and Invader LNA probes due to base pair breathing, which reveals nucleation sites for the formation of probe-target duplexes.[135] A related hypothesis has been formulated by Ly and coworkers to explain binding of single stranded γ-PNA to mixed-sequence dsDNA at low ionic strengths.[136] Subsequent studies have revealed that the free energy for molecular recognition of dsDNA by Invader LNA can be increased through changes in the linker chemistry between the pyrene moiety and the sugar skeleton of 2'-amino-α-L-LNA monomers.[137] The demanding synthesis of Invader LNA monomers is a potential limitation of this mixed-sequence dsDNA-targeting technology.[60,67] Gratifyingly, O2'-alkylated RNA and N2'-functionalized 2'-amino-DNA monomers have very recently been established as structural and functional analogs of Invader LNA monomers, which are synthetically more easily accessible.[138] The potential of Invader LNA for targeting of biologically relevant mixed-sequence dsDNA under physiological conditions is underscored by their ability to reduce RNA-formation in *in vitro* transcription assays.[139] Similar results have been observed with short "Invader LNA-like" probes modified with INA monomer **44** (Fig. 19) even though less free energy is available for dsDNA-targeting, presumably due to the high flexibility of **44**.[140]

8. Summary and Perspective

Pyrene-functionalized ONs (PFOs) are valuable model systems for fundamental studies of nucleic acid structures due to their straightforward synthetic manipulation, microenvironment-sensitive fluorescence, π-stacking ability and propensity for intercalation into DNA duplexes. An large number of pyrene-functionalized nucleotide monomers has emerged over the past ~10 years leading to major advances towards a) generation of self-assembled helical chromophore arrays, b) sensitive detection of DNA/RNA targets and discrimination of single nucleotide polymorphisms (SNPs), and c) sequence-unrestricted targeting of dsDNA. The majority of these advances have been predicated by the development of pyrene-functionalized monomers with low inherrent flexibility and, putatively, high positional control of the pyrene moiety (e.g., short linkers; conformationally restricted sugar moieties). The following key examples underline this point: a) the extensive pyrene arrays obtained with duplexes between RNA strands and 2'-*O*-methyl RNA probes that are sequentially modified with 2'-*O*-(pyren-1-yl)methyluridine **21** monomers, rely on the preference of pyrene moieties to adopt non-intercalating binding modes in *A*-type duplexes (Fig. 7)[71]; b) the extraordinary high fluorescence emission quantum yields of duplexes between Glowing LNA and complementary DNA/RNA targets (Φ_F up to 0.99) are a consequence of the conformationally locked bicyclic skeleton and the short amide linkage of monomer **37** working in concert to rigidly position the pyrene moiety in the non-quenching minor groove (Fig. 5, Table 1);[90–91] and c) the ability of double-stranded Invader LNA to spontanously dissociate and bind to mixed-sequence dsDNA targets under physiological and non-denaturing conditions is related to the fact that intercalators linked to the N2'-position of 2'-amino-α-L-LNA are preorganized to point toward the duplex core (Fig. 6 and 20).[134–135] Future studies on PFOs would greatly benefit from NMR or X-ray characterization in order to more confidently link the position of the chromophore with observed physical properties and to guide rational design of new monomers with enabling functions.

The proof-of-principle studies highlighted herein underline the many potential applications of PFOs within nucleic acid based diagnostics, therapeutics and materials science. Several challenges remain, e.g., development of highly sensitive and discriminating SNP-typing probes that can: i) be used against a wide range of targets regardless of sequence context, ii) be used for in vivo applications, and iii) compete with large-scale SNP-typing methodologies on cost, sample throughput, and/or sensitivity/specificity.[141] Moreover, realization of sequence-unrestricted dsDNA targeting would not only provide a tool for modulation of gene expression and gene manipulation, but also pave the way toward detection of dsDNA target regions by fluorescence in situ hybridization (FISH) at non-denaturing conditions or even in living cells. An occasionally discussed drawback of pyrene is its blue-light excitation which can lead to high levels of cellular autofluorescence and damage to cells and assays. While development of chromophores with red-shifted emission characteristics certainly is desirable, it should be kept in mind that pyrene-functionalized probes displaying high fluorescence emission quantum yields can be coupled to milder and potentially less damaging excitation sources.

The highlighted developments of PFOs, in concert with the considerable advances in structural DNA nanobiotechnology[68] and bioconjugation techniques,[142] set the stage for a merger of these areas to generate self-assembled functional nanomaterials.[143] For example, chemically modified DNA nanogrids lend themselves as supramolecular scaffolds for organization of chromophores for development of light harvesting complexes. PFOs will undoubtedly continue to play important roles as model systems and key components of such functional nanomaterials.

Acknowledgments

Nucleic acid oriented research in the Hrdlicka laboratory is supported by Award Number R01 GM088697 from the National Institute of General Medical Sciences, National Institutes of Health; Idaho NSF EPSCoR; University of Idaho Biological Applications of Nanotechnology (BANTech) Center; Institute of Translational Health Sciences (ITHS) (supported by grants UL1 RR025014, KL2 RR025015, and TL1 RR025016 from the NIH National Center for Research Resources); NIH Grant Number P20 RR016454 from the INBRE Program of the National Center for Research Resources; and the United States Department of Agriculture (award 2009-34479-19833).

Notes and references

1. Kashida H, Liang XG, Asanuma H. Curr. Org. Chem. 2009; 13:1065–1084.
2. Filichev VV, Pedersen EB. Wiley Encyclopedia of Chemical Biology. 2009; 1:493–524.
3. Malinovskii VL, Wenger D, Häner R. Chem. Soc. Rev. 2010; 39:410–422. [PubMed: 20111767]
4. Guckian KM, Schweitzer BA, Ren RXF, Sheils CJ, Tahmassebi DC, Kool ET. J. Am. Chem. Soc. 2000; 122:2213–2222. [PubMed: 20865137]
5. Dougherty G, Pilbrow JR. Int. J. Biochem. 1984; 16:1179–1192. [PubMed: 6397369]
6. Lu XJ, Olson WK. Nucleic Acids Res. 2003; 31:5108–5121. [PubMed: 12930962]
7. Yao CX, Kraatz HB, Steer RP. Photochem. Photobiol. Sci. 2005; 4:191–199. [PubMed: 15696236]
8. Kalyanasundaram K, Thomas JK. J. Am. Chem. Soc. 1977; 99:2039–2044.
9. Manoharan M, Tivel KL, Zhao M, Nafisi K, Netzel TL. J. Phys. Chem. 1995; 99:17461–17472.
10. Seo YJ, Ryu JH, Kim BH. Org. Lett. 2005; 7:4931–4933. [PubMed: 16235925]
11. Østergaard ME, Kumar P, Baral B, Guenther DC, Anderson BA, Ytreberg FM, Deobald L, Paszczynski AJ, Sharma PK, Hrdlicka PJ. Chem. Eur. J. 2011; 17:3157–3165. [PubMed: 21328492]
12. Winnik FM. Chem. Rev. 1993; 93:587–614.
13. Amann N, Pandurski E, Fiebig T, Wagenknecht HA. Chem. Eur. J. 2002; 8:4877–4883. [PubMed: 12397589]
14. Valis L, Mayer–Enthart E, Wagenknecht HA. Bioorg. Med. Chem. Lett. 2006; 16:3184–3187. [PubMed: 16621544]

15. Raytchev M, Mayer E, Amann N, Wagenknecht HA, Fiebig T. ChemPhysChem. 2004; 5:706–712. [PubMed: 15179723]
16. Wanninger-Weiss C, Wagenknecht HA. Eur. J. Org. Chem. 2008:64–69.
17. Mayer E, Valis L, Wagner C, Rist M, Amann N, Wagenknecht HA. ChemBioChem. 2004; 5:865–868. [PubMed: 15174171]
18. Maeda H, Maeda T, Mizuno K, Fujimoto K, Shimizu H, Inouye M. Chem. Eur. J. 2006; 12:824–831. [PubMed: 16267869]
19. Astakhova IV, Korshun VA, Wengel J. Chem. Eur. J. 2008; 14:11010–11026. [PubMed: 18979465]
20. Matray TJ, Kool ET. J. Am. Chem. Soc. 1998; 120:6191–6192. [PubMed: 20852721]
21. Østergaard ME, Guenther DC, Kumar P, Baral B, Deobald L, Paszczynski AJ, Sharma PK, Hrdlicka PJ. Chem. Commun. 2010:4929–4931.
22. Heystek LE, Zhou HQ, Dande P, Gold B. J. Am. Chem. Soc. 1998; 120:12165–12166.
23. Znosko BM, Barnes TW, krugh TR, Turner DH. J. Am. Chem. Soc. 2003; 125:6090–6097. [PubMed: 12785839]
24. Kottysch T, Ahlborn C, Brotzel F, Richert C. Chem. Eur. J. 2004; 10:4017–4028. [PubMed: 15316994]
25. Skorobogatyi MV, Malakhov AD, Pchelintseva AA, Turban AA, Bondarev SL, Korshun VA. ChemBioChem. 2006; 7:810–816. [PubMed: 16572492]
26. Okamoto A, Kanatani K, Saito I. J. Am. Chem. Soc. 2004; 126:4820–4827. [PubMed: 15080686]
27. Bag SS, Kundu R, Matsumoto K, Saito Y, Saito I. Bioorg. Med. Chem. Lett. 2010; 20:3227–3230. [PubMed: 20452214]
28. Saito Y, Hanawa K, Motegi K, Omoto K, Okamoto A, Saito I. Tetrahedron Lett. 2005; 46:7605–7608.
29. Seela F, Zulauf M. Helv. Chim. Acta. 1999; 82:1878–1898.
30. Saito Y, Miyauchi Y, Okamoto A, Saito I. Chem. Commun. 2004:1704–1705.
31. Seela F, Ingale SA. J. Org. Chem. 2010; 75:284–295. [PubMed: 20000692]
32. Grünefeld P, Richert C. J. Org. Chem. 2004; 69:7543–7551. [PubMed: 15497980]
33. Dohno C, Saito I. ChemBioChem. 2005; 6:1075–1081. [PubMed: 15852333]
34. Bryld T, Højland T, Wengel J. Chem. Commun. 2004:1064–1065.
35. Yamana K, Iwase R, Furutani S, Tsuchida H, Zako H, Yamaoka T, Murakami A. Nucleic Acids Res. 1999; 27:2387–2392. [PubMed: 10325429]
36. Yamana K, Zako H, Asazuma K, Iwase R, Nakano H, Murakami A. Angew. Chem. Int. Ed. 2001; 40:1104–1106.
37. Nakamura M, Fukunaga Y, Sasa K, Ohtoshi Y, Kanaori K, Hayashi H, Nakano H, Yamana K. Nucleic Acids Res. 2005; 33:5887–5895. [PubMed: 16237124]
38. Korshun VA, Stetsenko DA, Gait MJ. J. Chem. Soc. Perkin. Trans. 2002; 1:1092–1104.
39. Dioubankova NN, Malakhov AD, Shenkarev ZO, Korshun VA. Tetrahedron. 2004; 60:4617–4626.
40. Dioubankova NN, Malakhov AD, Stetsenko DA, Gait MJ, Volynsky PE, Efremov RG, Korshun VA. ChemBioChem. 2003; 4:841–847. [PubMed: 12964158]
41. Astakhova IV, Malakhov AD, Stepanova IA, Ustinov AV, Bondarey SL, Paramonov AS, Korshun VA. Bioconjugate Chem. 2007; 18:1972–1980.
42. Kalra N, Parlato MC, Parmar VS, Wengel J. Bioorg. Med. Chem. Lett. 2006; 16:3166–3169. [PubMed: 16621554]
43. Kalra N, Babu BR, Parmar VS, Wengel J. Org. Biomol. Chem. 2004; 2:2885–2887. [PubMed: 15480448]
44. Ratje, RL.; Anderson, BA.; Hrdlicka, PJ. unpublished results
45. Koshkin AA, Singh SK, Nielsen P, Rajwanshi VK, Kumar R, Meldgaard M, Olsen CE, Wengel J. Tetrahedron. 1998; 54:3607–3630.
46. Obika S, Nanbu D, Hari Y, Andoh J, Morio K, Doi T, Imanishi T. Tetrahedron Lett. 1998; 39:5401–5404.

47. Petersen M, Nielsen CB, Nielsen KE, Jensen GA, Bondensgaard K, Singh SK, Rajwanshi VK, Koshkin AA, Dahl BM, Wengel J, Jacobsen JP. J. Mol. Recognit. 2000; 13:44–53. [PubMed: 10679896]
48. Nielsen JT, Arar K, Petersen M. Nucleic Acids Res. 2006; 34:2006–2014. [PubMed: 16614450]
49. Konorov SO, Schulze HG, Addison CJ, Haynes CA, Blades MW, Turner RFB. J. Raman Spectrosc. 2009; 40:1162–1171.
50. Petersen M, Bondensgaard K, Wengel J, Jacobsen JP. J. Am. Chem. Soc. 2002; 124:5974–5982. [PubMed: 12022830]
51. Nielsen KE, Spielmann HP. J. Am. Chem. Soc. 2005; 127:15273–15282. [PubMed: 16248670]
52. Koch, T.; Ørum, H. Antisense Drug Technology – Principles, Strategies, and Applications. 2nd ed. Crooke, ST., editor. CRC Press; Boca Raton: 2008. p. 519-564.
53. Sørensen MD, Kværnø L, Bryld T, Håkansson AE, Verbeure B, Gaubert G, Herdewijn P, Wengel J. J. Am. Chem. Soc. 2002; 124:2164–2176. [PubMed: 11878970]
54. Nielsen KME, Petersen M, Håkansson AE, Wengel J, Jacobsen JP. Chem. Eur. J. 2002; 8:3001–3009. [PubMed: 12489231]
55. Nielsen JT, Stein P, Petersen M. Nucleic Acids Res. 2003; 31:5858–5867. [PubMed: 14530434]
56. Fluiter K, Frieden M, Vreijling J, Rosenbohm C, De Wissel MB, Christensen SM, Koch T, Ørum H, Baas F. ChemBioChem. 2005; 6:1104–1109. [PubMed: 15861430]
57. Petersen M, Wengel J. Trends Biotechnol. 2003; 21:74–81. [PubMed: 12573856]
58. Kaur H, Babu BR, Maiti S. Chem. Rev. 2007; 107:4672–4697. [PubMed: 17944519]
59. Singh SK, Kumar R, Wengel J. J. Org. Chem. 1998; 63:10035–10039.
60. Kumar TS, Madsen AS, Wengel J, Hrdlicka PJ. J. Org. Chem. 2006; 71:4188–4201. [PubMed: 16709060]
61. Babu BR, Prasad AK, Trikha S, Thorup N, Parmar VS, Wengel J. J. Chem. Soc. Perkin Trans. 2002; 1:2509–2519.
62. Raunak, B. R. Babu; Sørensen, MD.; Parmar, VS.; Harrit, NH.; Wengel, J. Org. Biomol. Chem. 2004; 2:80–89. [PubMed: 14737663]
63. Verhagen C, Bryld T, Raunkær M, Vogel S, Buchalova K, Wengel J. Eur. J. Org. Chem. 2006:2538–2548.
64. Østergaard ME, Kumar P, Baral B, Raible DJ, Kumar TS, Anderson BA, Guenther DC, Deobald L, Paszczynski AJ, Sharma PK, Hrdlicka PJ. ChemBioChem. 2009; 10:2740–2743. [PubMed: 19810078]
65. Kumar, P.; hrdlicka, PJ. unpublished results
66. Sørensen MD, Petersen M, Wengel J. Chem. Commun. 2003:2130–2131.
67. Kumar TS, Madsen AS, Østergaard ME, Sau SP, Wengel J, Hrdlicka PJ. J. Org. Chem. 2009; 74:1070–1081. [PubMed: 19108636]
68. Aldaye FA, Palmer AL, Sleiman HF. Science. 2008; 321:1795–1799. [PubMed: 18818351]
69. Varghese R, Wagenknecht HA. Chem. Commun. 2009:2615–2624.
70. Nguyen TN, Brewer A, Stulz E. Angew. Chem. Int. Ed. 2009; 48:1974–1977.
71. Nakamura M, Shimomura Y, Ohtoshi Y, Sasa K, Hayashi H, Nakano H, Yamana K. Org. Biomol. Chem. 2007; 5:1945–1951. [PubMed: 17551644]
72. Hrdlicka PJ, Babu BR, Sørensen MD, Wengel J. Chem. Commun. 2004:1478–1479.
73. Astakhova IV, Lindegaard D, Korshun VA, Wengel J. Chem. Commun. 2010; 46:8362–8364.
74. Lindegaard D, Babu BR, Wengel J. Nucleos. Nucleot. Nucleic Acids. 2005; 24:679–681.
75. Nakamura M, Murakami Y, Sasa K, Hayashi H, Yamana K. J. Am. Chem. Soc. 2008; 130:6904–6905. [PubMed: 18473465]
76. Mayer-Enthart E, Wagenknecht HA. Angew. Chem. Int. Ed. 2006; 45:3372–3375.
77. Barbaric J, Wagenknecht HA. Org. Biomol. Chem. 2006; 4:2088–2090. [PubMed: 16729121]
78. Tanaro K, Shionoya M. Coord. Chem. Rev. 2007; 251:2732–2742.
79. Kumar TS, Madsen AS, Østergaard ME, Wengel J, Hrdlicka PJ. J. Org. Chem. 2008; 73:7060–7066. [PubMed: 18710289]

80. Häner R, Garo F, Wenger D, Malinovskii VL. J. Am. Chem. Soc. 2010; 132:7466–7471. [PubMed: 20459110]
81. Chiba J, Takeshima S, Mishima K, Maeda H, Nanai Y, Mizuno K, Inouye M. Chem. Eur. J. 2007; 13:8124–8130. [PubMed: 17607793]
82. Teo YN, Wilson JN, Kool ET. J. Am. Chem. Soc. 2009; 131:3923–3933. [PubMed: 19254023]
83. Kubista M, Andrade JM, Bengtsson M, Forootan A, Jonak J, Lind K, Sindelka R, Sjöback R, Sjögreen B, Strömbom L, Ståhlberg A, Zorix N. Mol. Asp. Med. 2006; 27:95–125.
84. Mahara A, Iwase R, Sakamoto T, Yamaoka T, Yamana K, Murakami A. Bioorg. Med. Chem. 2003; 11:2783–2790. [PubMed: 12788352]
85. Bratu DP, Cha BJ, Mhlanga MM, Kramer FR, Tyagi S. Proc. Natl. Acad. Sci. U. S. A. 2003; 100:13308–13313. [PubMed: 14583593]
86. Sobrino B, Brion M, Carracedo A. Forensic Sci. Int. 2005; 154:181–194. [PubMed: 16182964]
87. Alocilja EC, Radke SM. Biosens. Bioelectron. 2003; 18:841–846. [PubMed: 12706600]
88. Asseline U. Curr. Org. Chem. 2006; 10:491–518.
89. Wang G, Bobkov GV, Mikhailov SN, Schepers G, Van Aerschot A, Rozenski J, Van der Auweraer M, Herdewijn P, De Feyter S. ChemBioChem. 2009; 10:1175–1185. [PubMed: 19373795]
90. Hrdlicka PJ, Babu BR, Sørensen MD, Harrit N, Wengel J. J. Am. Chem. Soc. 2005; 127:13293–13299. [PubMed: 16173760]
91. Østergaard ME, Cheguru P, Papasani MR, Hill RA, Hrdlicka PJ. J. Am. Chem. Soc. 2010; 132:14221–14228. [PubMed: 20845923]
92. Østergaard ME, Maity J, Babu BR, Wengel J, Hrdlicka PJ. Bioorg. Med. Chem. Lett. 2010; 20:7265–7268. [PubMed: 21071224]
93. Honcharenko D, Zho C, Chattopadhyaya J. J. Org. Chem. 2008; 73:2829–2842. [PubMed: 18331060]
94. Okamoto A, Saito Y, Saito I. J. Photochem. Photobiol. C. 2005; 6:108–122.
95. Dodd DW, Hudson RHE. Mini–Rev. Org. Chem. 2009; 6:378–391.
96. Kim S, Misra A. Annu. Rev. Biomed. Eng. 2007; 9:289–320. [PubMed: 17391067]
97. Hwang GT, Seo YJ, Kim SJ, Kim BH. Tetrahedron Lett. 2004; 45:3543–3546.
98. Okamoto A, Ochi Y, Saito I. Chem. Commun. 2005:1128–1130.
99. Yoshida Y, Niwa K, Yamada K, Tokeshi M, Baba Y, Saito Y, Okamoto A, Saito I. Chem. Lett. 2010; 39:116–117.
100. Okamoto A, Tainaka K, Ochi Y, Kanatani K, Saito I. Mol. Biosyst. 2006; 2:122–126. [PubMed: 16880929]
101. Saito Y, Bag SS, Kusakabe Y, Nagai C, Matsumoto K, Mizuno E, Kodate S, Suzuka I, Saito I. Chem. Commun. 2007:2133–2135.
102. Mahara A, Iwase R, Sakamoto T, Yamana K, Yamaoka T, Murakami A. Angew. Chem. Int. Ed. 2002; 41:3648–3650.
103. Umemoto T, Hrdlicka PJ, Babu BR, Wengel J. ChemBioChem. 2007; 8:2240–2248. [PubMed: 17979173]
104. Kolpashchikov DM. Chem. Rev. 2010; 110:4709–4723. [PubMed: 20583806]
105. Paris PL, Langenhan JM, Kool ET. Nucleic Acids Res. 1998; 26:3789–3793. [PubMed: 9685497]
106. Bichenkova EV, Sardarian A, Savage HE, Rogert C, Douglas KT. Assay Drug Devel. Technol. 2005; 3:39–46. [PubMed: 15798394]
107. Marti AA, Li XX, Jockusch S, Li ZM, Raveendra B, Kalachikov S, Russo JJ, Morozova I, Puthanveettil SV, Ju JY, Turro NJ. Nucleic Acids Res. 2006; 34:3161–3168. [PubMed: 16769776]
108. Bichenkova EV, Gbaj A, Walsh L, Savage HE, Rogert C, Sardarian AR, Etchells LL, Douglas KT. Org. Biomol. Chem. 2007; 5:1039–1051. [PubMed: 17377657]
109. Kumar TS, Wengel J, Hrdlicka PJ. ChemBioChem. 2007; 8:1122–1125. [PubMed: 17551917]
110. Christensen UB, Pedersen EB. Helv. Chim. Acta. 2003; 86:2090–2097.
111. Wang K, Tang Z, Yang CJ, Kim Y, Fang X, Li W, Wu Y, Medley CD, Cao Z, Li J, Colon P, Lin H, Tan W. Angew. Chem. Int. Ed. 2009; 48:856–870.

112. Venkatesan N, Seo YJ, Kim BH. Chem. Soc. Rev. 2008; 37:648–663. [PubMed: 18362974]
113. Saito Y, Mizuno E, Bag SS, Suzuka I, Saito I. Chem. Commun. 2007:4492–4494.
114. Saito Y, Shinohara Y, Bag SS, Takeuchi Y, Matsumoto K, Saito I. Tetrahedron. 2009; 65:934–939.
115. Fujmoto K, Shimizu H, Inouye M. J. Org. Chem. 2004; 69:3271–3275. [PubMed: 15132531]
116. Seo YJ, Hwang GT, Kim BH. Tetrahedron Lett. 2006; 47:4037–4039.
117. Matsumoto K, Shinohara Y, Bag SS, Takeuchi Y, Morii T, Saito Y, Saito I. Bioorg. Med. Chem. Lett. 2009; 19:6392–6395. [PubMed: 19828314]
118. Conlon P, Yang CJ, Wu Y, Chen Y, Martinez K, Kim Y, Stevens N, Marti AA, Jockusch S, Turro NJ, Tan W. J. Am. Chem. Soc. 2008; 130:336–342. [PubMed: 18078339]
119. Varghese R, Wagenknecht HA. Org. Biomol. Chem. 2010; 8:526–528. [PubMed: 20090965]
120. Smalley MK, Silverman SK. Nucleic Acids Res. 2006; 34:152–166. [PubMed: 16401611]
121. Seo YJ, Lee IJ, Yi JW, Kim BH. Chem. Commun. 2007:2817–2819.
122. Alberti P, Bourdoncle A, Sacca B, Lacroix L, Mergny JL. Org. Biomol. Chem. 2006; 4:3383–3391. [PubMed: 17036128]
123. Beuck C, Singh I, Bhattacharya A, Heckler W, Parmar VS, Seitz O, Weinhold E. Angew. Chem. Int. Ed. 2003; 42:3958–3960.
124. Krosky DJ, Song F, Stivers JT. Biochemistry. 2005; 44:5949–5959. [PubMed: 15835884]
125. Jeong HS, Kang S, Lee JY, Kim BH. Org. Biomol. Chem. 2009; 7:921–925. [PubMed: 19225675]
126. Crooke, ST.; Vickers, T.; Lima, W.; Wu, H. Antisense Drug – Technology – Principles, Strategies and Applications. 2nd ed.. Crooke, ST., editor. CRC Press; Boca Raton: 2008. p. 3-46.
127. Rogers FA, Lloyd JA, Glazer PM. Curr. Med. Chem. – Anti–Cancer Agents. 2005; 5:319–326.
128. Ghosh I, Stains CI, Ooib AT, Segal DJ. Mol. Biosyst. 2006; 2:551–560. [PubMed: 17216036]
129. Duca M, Vekhoff P, Oussedik K, Halby L, Arimondo PB. Nucleic Acids Res. 2008; 36:5123–5138. [PubMed: 18676453]
130. Simon P, Cannata F, Concordet JP, Giovannangeli C. Biochimie. 2008; 90:1109–1116. [PubMed: 18460344]
131. Filichev VV, Pedersen EB. J. Am. Chem. Soc. 2005; 127:14849–14858. [PubMed: 16231939]
132. Schneider UV, Mikkelsen ND, Jøhnk N, Okkels LM, Westh H, Lisby G. Nucleic Acids Res. 2010; 38:4394–4403. [PubMed: 20338879]
133. Paramasivam M, Cogoi S, Filichev VV, Bomholt N, Pedersen EB, Xodo LE. Nucleic Acids Res. 2008; 36:3494–3507. [PubMed: 18456705]
134. Hrdlicka PJ, Kumar TS, Wengel J. Chem. Commun. 2005:4279–4281.
135. Sau SP, Kumar TS, Hrdlicka PJ. Org. Biomol. Chem. 2010; 8:2028–2036. [PubMed: 20401378]
136. Chenna V, Rapireddy S, Sahu B, Ausin C, Pedroso E, Ly DH. ChemBioChem. 2008; 9:1–4.
137. Sau, SP.; Hrdlicka, PJ. unpublished results
138. Hrdlicka, PJ., et al. unpublished results
139. Papasani, MR.; Hrdlicka, PJ.; Hill, RA., et al. unpublished results
140. Filichev VV, Vester B, Hansen LH, Pedersen EB. Nucleic Acids Res. 2005; 33:7129–7137. [PubMed: 16377781]
141. LaFramboise T. Nucleic Acids Res. 2009; 37:4181–4193. [PubMed: 19570852]
142. Weisbrod SH, Marx A. Chem. Commun. 2008:5675–5685.
143. Wengel J. Org. Biomol. Chem. 2004; 2:277–280. [PubMed: 14747851]
144. Nakamura M, Ohtoshi Y, Yamana K. Chem. Commun. 2005:5163–5165.

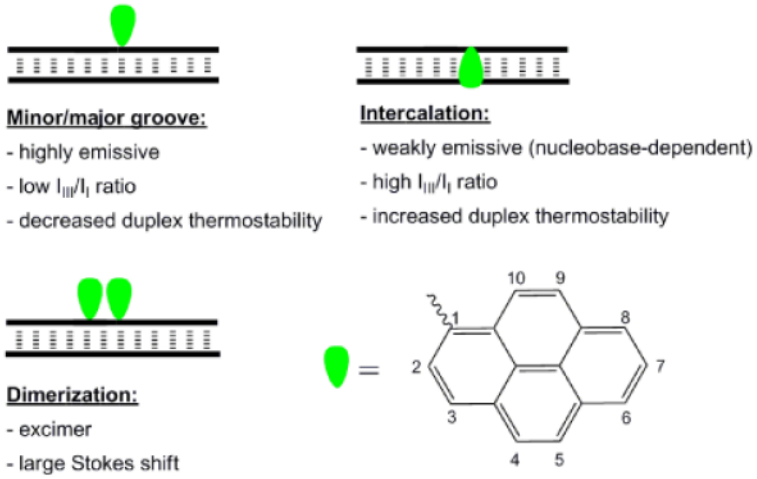

Fig. 1.
Position-dependent pyrene characteristics in nucleic acid duplexes.

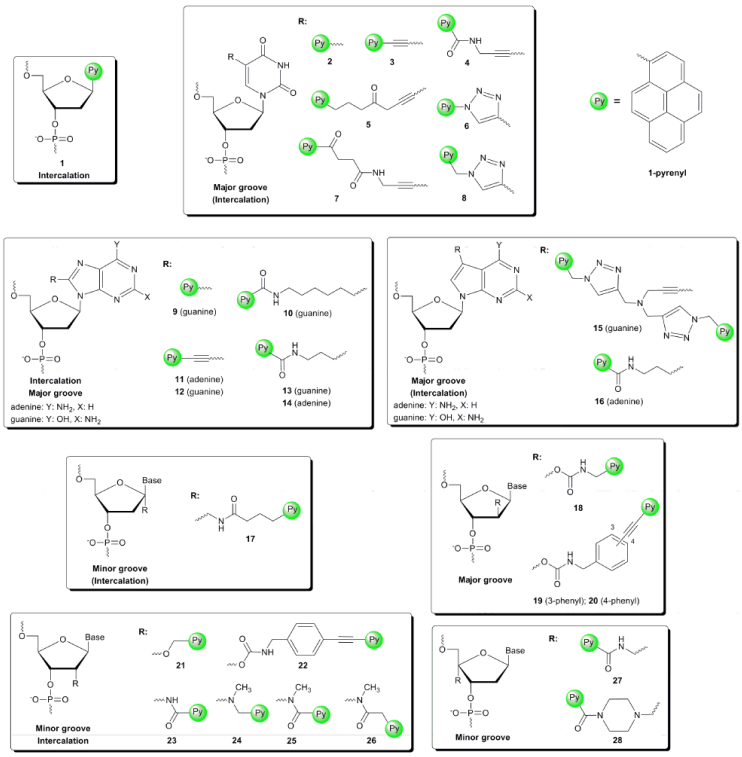

Fig. 2.

Pyrene-functionalized monomers and anticipated location of the pyrene moiety in nucleic acid duplexes.

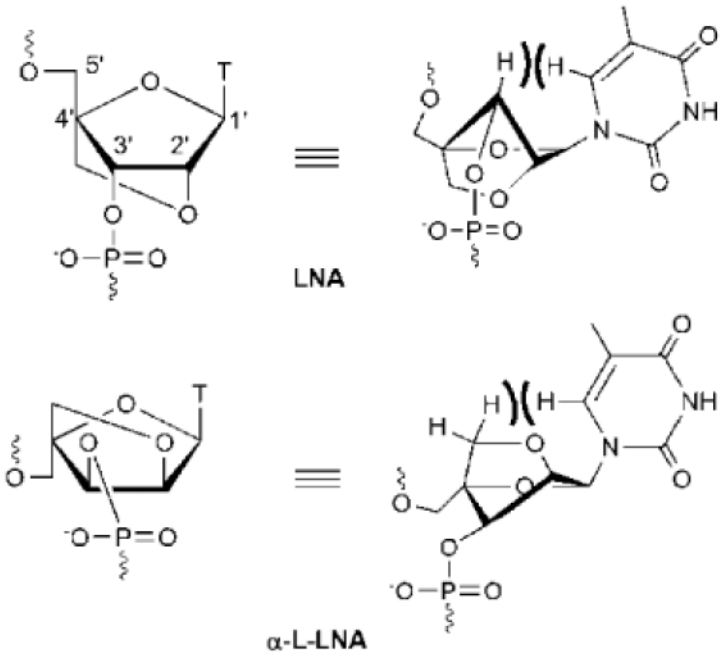

Fig. 3.
Structure of LNA-T and α-L-LNA-T monomers. Numbering of sugar ring carbons is shown for LNA.

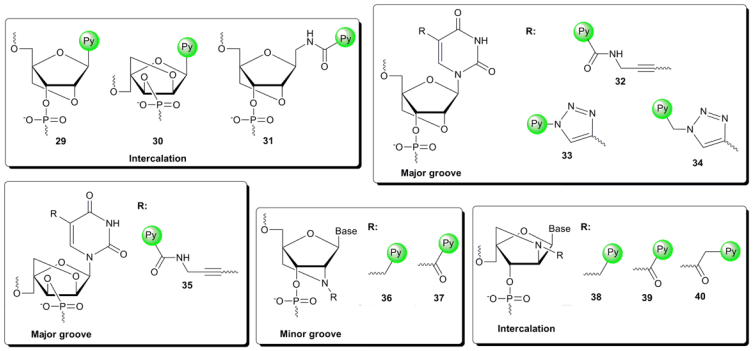

Fig. 4.
Pyrene-functionalized LNAs and anticipated location of the pyrene moiety in nucleic acid duplexes.

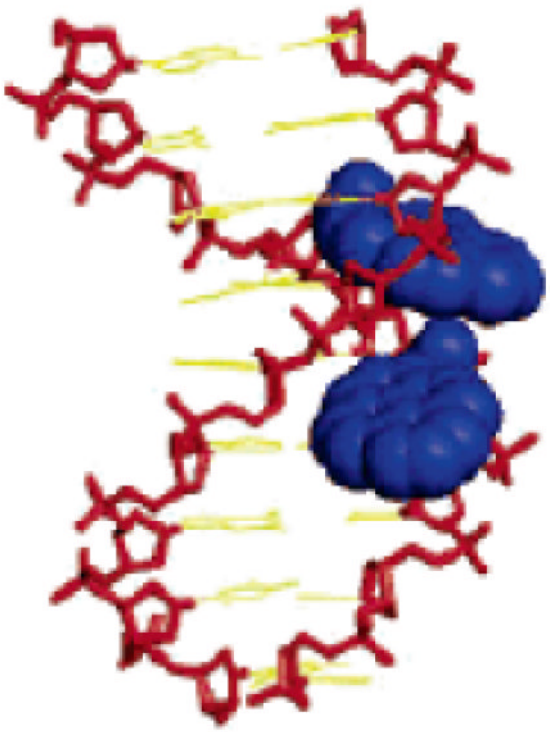

Fig. 5.
Placement of pyrene moieties in the minor groove using N2'-functionalized 2'-amino-LNA. Molecular modelling structure of duplex between 5'-d(GCA **37**A**37** CAC) and 3'-d(CGT ATA GTG). Monomer **37**: 2'-*N*-(pyren-1-yl)carbonyl-2'-amino-LNA-T. (Reproduced with permission from ref. 90. Copyright 2005 American Chemical Society).

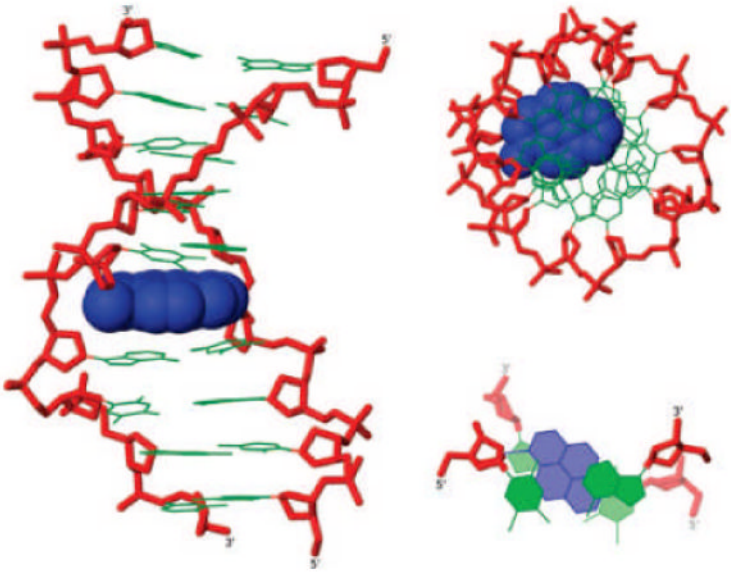

Fig. 6.

Placement of pyrene moieties in the duplex core using N2'-functionalized 2'-amino-α-L-LNA. Different representations of molecular modelling structure of duplex between 5'-d(GTG A**38**A TGC) and 3'-d(CAC TAT ACG). Monomer **38**: 2'-*N*-(pyren-1-yl)methyl-2'-amino-α-L-LNA-T. (Reproduced with permission from ref. 67. Copyright 2009 American Chemical Society).

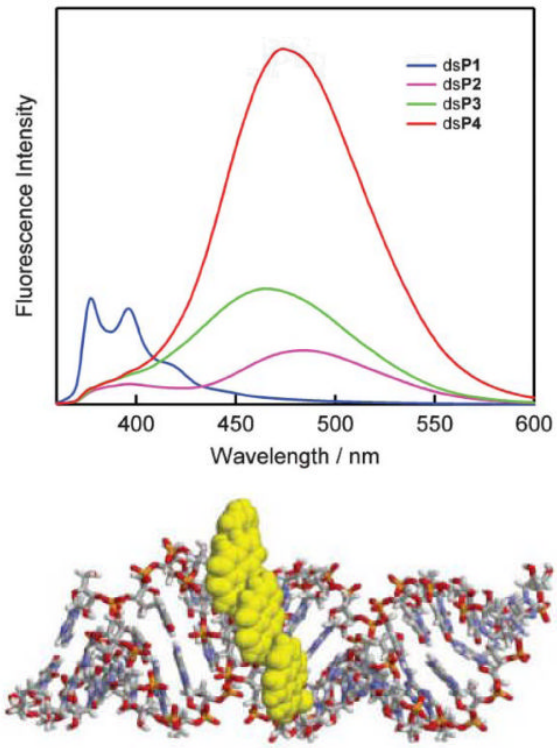

Fig. 7.

Formation of pyrene arrays in the minor groove using 2'-*O*-(pyren-1-yl)methyluridine **21** monomers. *Upper*: fluorescence emission spectra of duplexes between 19-mer 2'-*O*-methyluridine strands centrally modified with 1–4 sequential **21** monomers and complementary RNA (ds**P1**–ds**P4**, λ_{ex} = 350 nm). (Reproduced with permission from ref. 144 Copyright 2005 RSC) *Lower*: molecular modelling structure of ds**P4**. (Reproduced with permission from ref. 71. Copyright 2007 RSC Publishing).

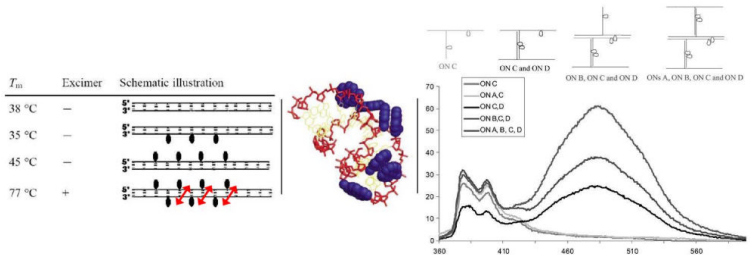

Fig. 8.

Formation of pyrene interstrand zipper arrays using 2'-N-(pyren-1-yl)methyl-2'-amino-LNA monomer **36**. *Left*: T_m-values and fluorescence characteristics of DNA duplexes modified with monomer **36**. Arrows indicate −1 zipper orientation.[63] *Middle*: molecular modelling structure of duplex with three −1 interstrand arrangements of monomer **36** (T_m = 77 °C). (Adapted from ref. 72. Copyright 2004 RSC Publishing). *Right*: fluorescence emission spectra illustrating stepwise self-assembly of higher order nucleic acid structures (using monomer **36**). (Adapted with permission from ref. 74. Copyright 2005 Taylor & Francis).

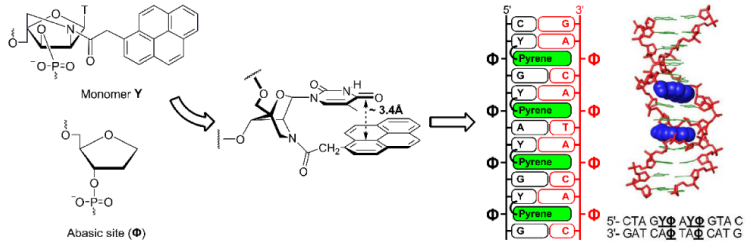

Fig. 9.

Left: illustration of pyrene array formation in the duplex core using 5'-(**Y**Φ):3'-(**A**Φ)-units where **Y** denotes 2'-*N*-(pyren-1-yl)acetyl-2'-amino-α-L-LNA-T monomer **40** and monomer Φ is an abasic site analog. *Right*: molecular modelling structure of a 13-mer DNA duplex containing two separated 5'-(**Y**Φ): 3'-(**A**Φ)-units. (Adapted with permission from ref. 79. Copyright 2008 American Chemical Society).

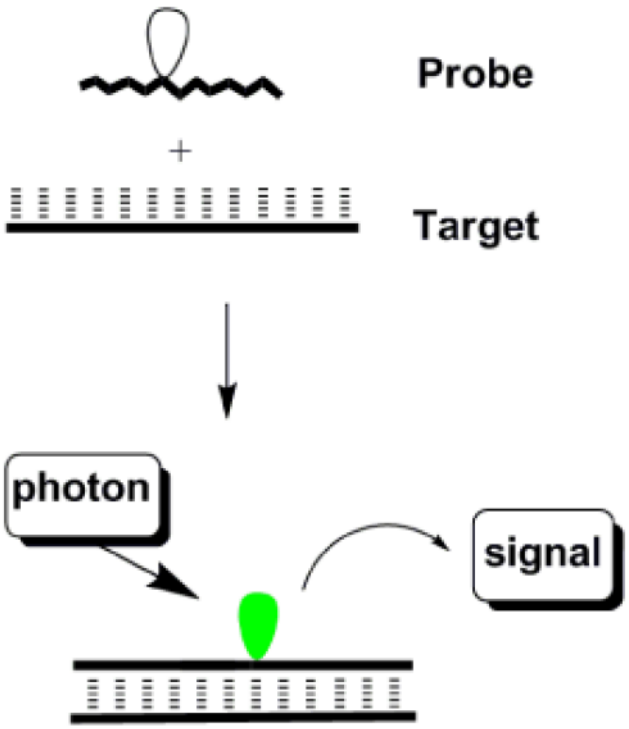

Fig. 10.
Principle of hybridization probes. White and green droplets represent silent and emissive fluorophore.

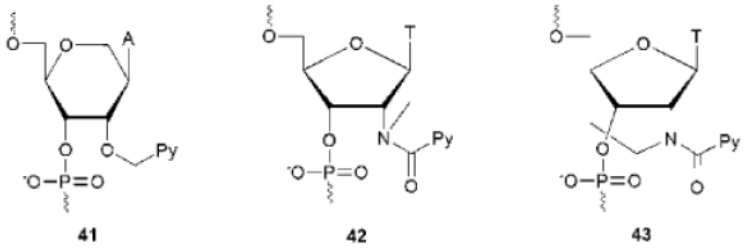

41 42 43

Fig. 11.
Pyrene-functionalized monomers utilized in hybridization probes. Py = pyren-1-yl.

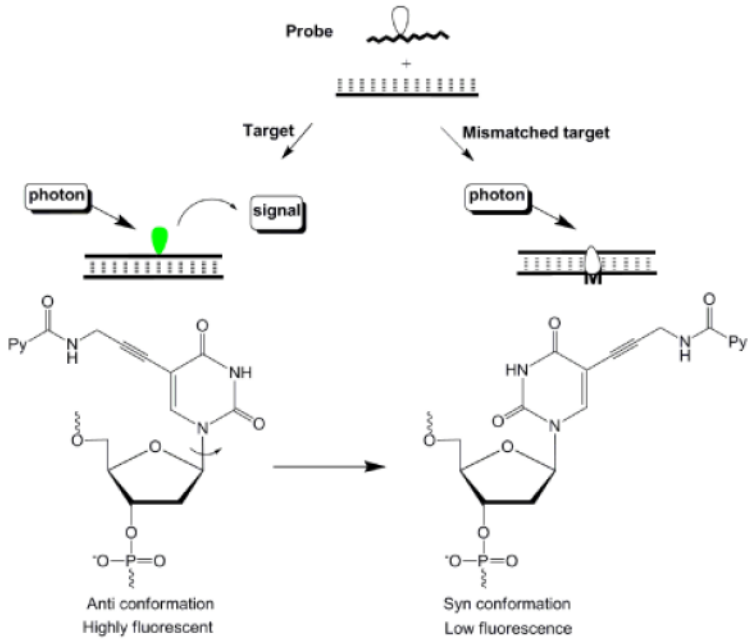

Fig. 12.
Principle of BDF probes.

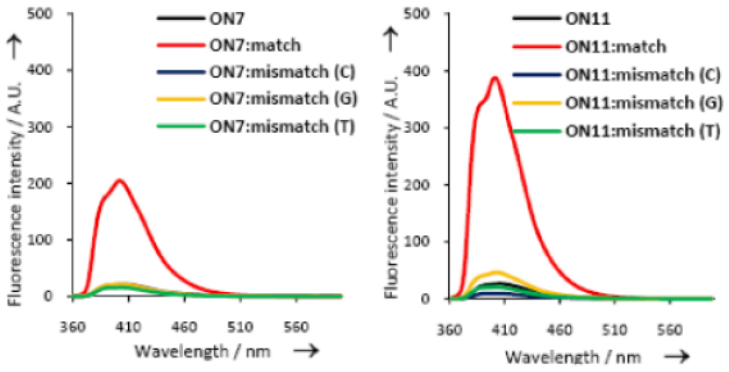

Fig. 13.

SNP discrimination using C5-[3-(1-pyrenecarboxamido)propynyl] DNA/LNA monomers. Fluorescence emission spectra of 5'-d(CG CAA G**B**G AAC GC-3'), where **B** = DNA monomer **4** (**ON7**) or LNA monomer **32** (**ON11**), against complementary or singly mismatched DNA. (Reproduced with permission from ref. 11. Copyright 2011 Wiley).

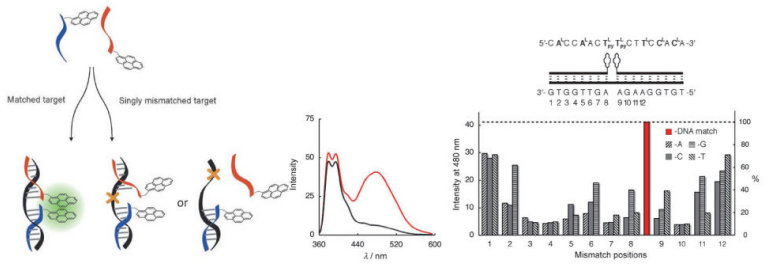

Fig. 14.

Left: principle of SNP-discrimination by excimer-forming dual probes. *Middle*: fluorescence emission spectra of LNA-based dual probes end-functionalized with monomer **36** and complementary (*red*) or singly mismatched DNA target (*black*). *Right*: probe/target sequences; discrimination of SNPs in positions 1–12 (λ_{em} = 480 nm). (Adapted with permission from ref. 103. Copyright 2007 Wiley).

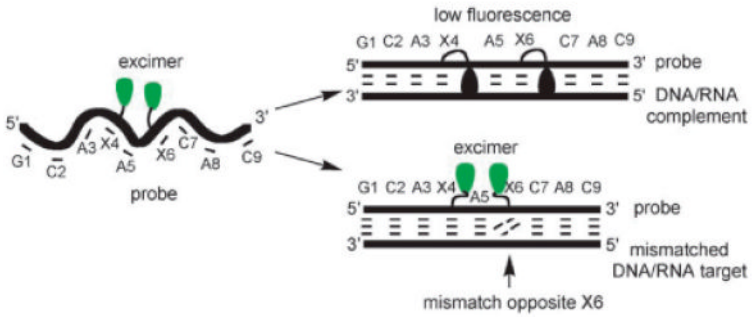

Fig. 15.

Principle of mismatch detection using doubly modified 2'-*N*-(pyren-1-yl)acetyl-2'-amino-α-L-LNA **40**. (Reproduced with permission from ref. 109. Copyright 2007 Wiley).

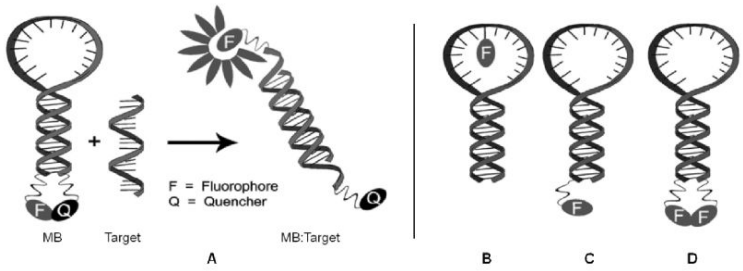

Fig. 16.

A: General principle of a conventional MB. B–D: Different quencher-free MB designs. (Adapted with permission from ref. 112. Copyright 2008 RSC Publishing).

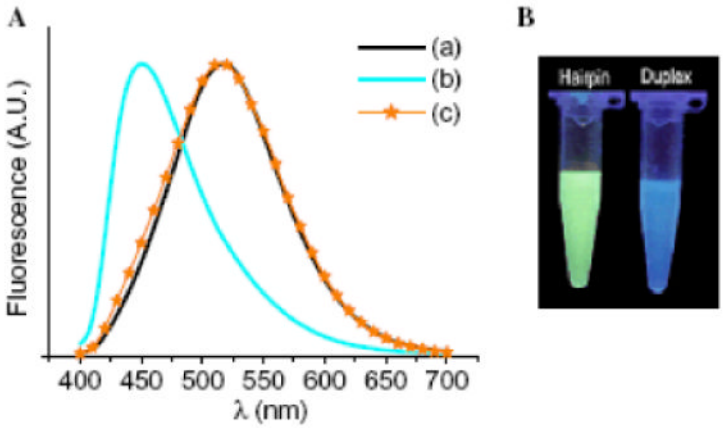

Fig. 17.

Excimer-forming MBs. *Left*: Fluorescence emission spectra (λ_{ex} = 386 nm) of (a) MB alone, (b) MB + complementary DNA and, (c) MB + singly mismatched DNA. *Right*: Optical detection of complementary DNA. MB sequence: 5'-d(GC**11** GAG AAG TTA GAA CCT ATG CTC **11**GC). (Reproduced with permission from ref. 116. Copyright 2006 Elsevier Ltd.).

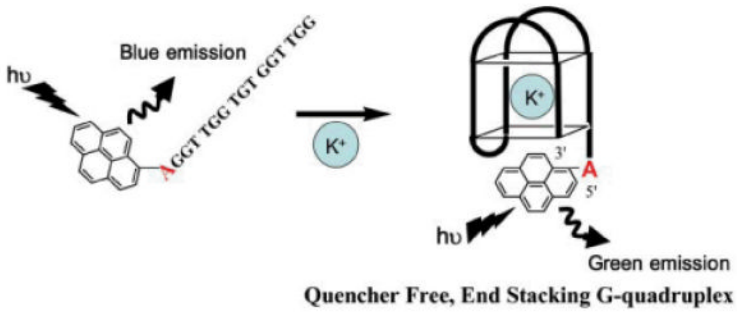

Fig. 18.

Fig. 18. Fluorescence signalling of quadruplex formation. (Reproduced with permission from ref. 121. Copyright 2007 RSC Publishing).

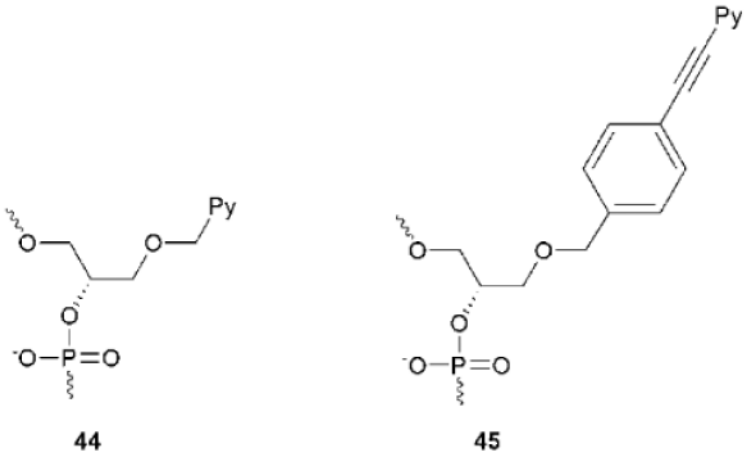

44 45

Fig. 19.
Non-nucleosidic monomers used for dsDNA-targeting.

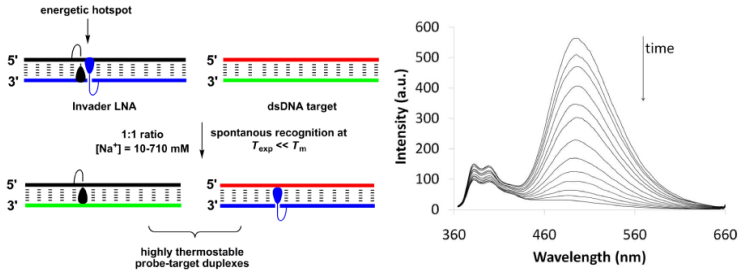

Fig. 20.

Left: illustration of the Invader LNA concept. *Right*: time course of steady-state fluorescence spectra upon addition of pre-annealed Invader LNA to pre-annealed isosequential dsDNA target (λ_{ex} = 335 nm, 20 °C). Invader LNA: 5'-d(GGT A**38**A TAT AGG C):3'-d(CCA TA**38** ATA TCC G) using monomer **38**. Isosequential dsDNA target: as for Invader LNA except **38** is placed by T. (Adapted from ref. 135. Copyright 2010 RSC Publishing).

Table 1

Thermal denaturation temperatures (T_m) and fluorescence quantum yields (Φ_F) of singly and doubly modified Glowing LNA probes in different backbone contexts and their duplexes with complementary DNA/RNA (**1X**, 5'-GCA T(U)A**37** CAC; **2X**, 5'-GCA **37**A**37** CAC). (Reproduced with permission from ref. 91. Copyright 2010 American Chemical Society).

	T_m (ΔT_m/mod)/°C		quantum yield (Φ_F)		
probe	**+DNA**	**+RNA**	**SSP**	**+DNA**	**+RNA**
DNA 1X	32.5 (+3.0)	33.0 (+6.0)	0.50	0.79	0.91
DNA 2X	40.5 (+5.5)	41.5 (+7.5)	0.27	0.81	0.70
PS-DNA 1X	24.0 (+3.5)	26.0 (+7.5)	0.50	0.64	0.66
PS-DNA 2X	32.0 (+6.0)	35.0 (+8.5)	0.20	0.61	0.62
RNA 1X	31.5 (+4.5)	42.5 (+4.5)	0.84	0.89	0.93
RNA 2X	38.0 (+5.5)	46.5 (+4.0)	0.16	0.85	0.89
O2'-Me 1X	31.0 (+5.0)	45.0 (+4.5)	1.00	0.97	0.98
O2'-Me 2X	20.0 (−3.0)	46.0 (+3.0)	0.14	0.68	0.86
LNA 1X	54.5 (−3.5)	64.0 (−5.0)	0.95	0.90	0.89
LNA 2X	49.0 (−4.5)	60.5 (−4.5)	0.72	0.92	0.84